

# **LOCATING THE HIP JOINT CENTRE USING ULTRASONIC TECHNIQUES**

Mona Tahvildar-Khazaneh



This thesis is submitted in partial fulfillment of the requirements for the degree of  
MSc in Biomedical Engineering  
August 13<sup>th</sup> 2013  
Department of Biomedical Engineering

## **Declaration**

This thesis is the result of the author's original research. It has been composed by the author and has not been previously submitted for examination which has led to the award of a degree.

The copyright of this thesis belongs to the author under the terms of the United Kingdom Copyright Acts as qualified by University of Strathclyde Regulation 3.50. Due acknowledgement must always be made of the use of any material contained in, or derived from, this thesis.

Signed:

Date: August 13<sup>th</sup> 2013



## **Acknowledgments**

I would like to express my gratitude to my supervisor, Mr. Stephanos Solomonidis, for all his guidance. His advice and enthusiasm were always welcomed and highly appreciated. I would also like to thank Dr. Oleg Davydov and Professor George Corner for their expertise and suggestions.

Lastly, I would like to thank my family for their unending encouragements. This thesis is dedicated to my parents who have given me the opportunity of an education from the best institutions around the world and who have supported me throughout my life.

*“Capacity without education is deplorable,  
and education without capacity is thrown away” - Saadi*

## **Abstract**

Locating the Hip Joint Centre (HJC) is crucial for gait analyses. These studies allow for precise calculation of both kinetic and kinematic parameters, which are required for determining the forces and moments around the hip. However, unlike the knee and ankle joints of the lower limb, which can be easily located due to their close proximity to the surface of the skin, the hip joint is situated deeply in the pelvis. The challenge of incorrectly locating the HJC is the incorporation of errors as great as 20% into the parameters needed for gait studies.

Although there have been developments in the approaches that are currently being used in locating the HJC, not much advancements have been made. Comparative studies between these methods have shown that the functional methods, which are based on sphere-fitting models, produce more accurate results than the predictive methods that are based on regression equation established from pelvic geometries. The underlying issue with using these methods is their incorporation of Soft Tissue Artifacts (STA). The use of alternative methods, such as medical imaging, for locating the HJC that have the ability to reduce errors associated with STA are promising techniques.

This study focused on the use of ultrasound for locating the HJC and attempted to compare the results to the functional methods currently used for verification. Although a direct comparison could not be made between these two methods, it is shown that the use of ultrasounds for locating the HJC reduces the incorporation of STA making it simpler to locate the HJC. However, a lot more investigation needs to be carried out in ultrasound image processing before they can be used as the new gold standard.

## Table of Contents

<b>1</b>	<b>Background</b>	<b>1</b>
1.1	Introduction	1
1.2	Aims	2
<b>2</b>	<b>Literature Review</b>	<b>3</b>
2.1	Principles of Ultrasound	3
2.1.1	Characterisation of Ultrasound waves	4
2.1.2	Ultrasonic Parameters	4
2.1.3	Detection of Ultrasound	6
2.1.4	Imaging Methods	8
2.2	Hip joint centre	10
2.2.1	Significance of The Hip Joint	10
2.2.2	Anatomy and Axis System	11
2.2.3	Challenges in Locating the HJC	13
2.3	Current Methods	17
2.3.1	Predictive Methods	17
2.3.2	Functional Methods	18
2.3.3	Validation Methods	19
2.4	Current Ultrasound techniques for locating the HJC	21
<b>3</b>	<b>Methodology</b>	<b>26</b>
3.1	Background	26
3.2	Subject Testing	27
3.3	Phantom and Tissue Mimicking Model	27
3.4	Ultrasound Imaging	28
3.5	Mimics Software	29
3.6	Experimental Design for Ultrasound Imaging	30
3.7	Functional Method verification	31
3.8	Motion Capture System	31
3.9	MATLAB Software	32
3.10	Experimental Design for the Vicon Motion Capture System	33
3.11	Data Acquisition	34
<b>4</b>	<b>Results and Discussion</b>	<b>36</b>
4.1	Ultrasound Imaging of the Phantom Model	36
4.1.1	Ultrasound Gel Coupling	36
4.1.2	Water Bath Submersion	37
4.2	Ultrasound Imaging of the Subject	39
4.3	Location of the HJC using Ultrasound Imaging	40
4.4	Functional Method Validation	43
4.4.1	Placement of Markers on the Subject's Skin	44
4.4.2	Placement of Markers on a Cotton Strap	46
4.5	Ultrasound and Functional Method Comparison	48

<b>5</b>	<b>Conclusion .....</b>	<b>50</b>
<b>6</b>	<b>Future Work .....</b>	<b>51</b>
6.1	Improvements in Ultrasonic Techniques .....	51
6.2	Improvements for Ultrasonic Image Processing .....	52
6.3	Improvements for Data Acquisition using Functional Methods .....	52
	<b>References .....</b>	<b>54</b>
	<b>Appendices .....</b>	<b>57</b>
	<b>Appendix A: University of Strathclyde’s Codes and Guidelines .....</b>	<b>57</b>
	Ethics Form .....	57
	Management Risk Assessment and Sponsorship.....	64
	Participant Information and Consent Forms .....	65
	E-mail: Nature of Participant .....	68
	<b>Appendix B: MATLAB code .....</b>	<b>69</b>
	<b>Appendix C: Ultrasound Image Modification .....</b>	<b>81</b>
	<b>Appendix D: Re-sizing Image MATLAB Code .....</b>	<b>83</b>

# 1 Background

## 1.1 Introduction

In order to determine accurately kinematic and kinetic data during studies of human motion, the location of the centre of rotation of various joints of the lower limb should be located as accurately as possible. Gait analysis, which is the study of human motion, is widely used as a diagnostic tool for identifying regions of pain, locations of movement restrictions, joint misalignments and weaknesses in muscles. These studies allow identification of corrective procedures to help relieve patients from pain. Although the knee and ankle joints can be determined reasonably well by palpation, the hip joint centre (HJC) is difficult to locate as it is situated deeply in the pelvis surrounded by large volumes of soft tissue.

Predictive and functional methods are currently the two main approaches that are used for determining the HJC. A comparative study carried out by Ehrig *et al* [27], has proved that neither of these methods are accurate; errors as great as 20% have been shown to be incorporated in calculating the HJC using these methods. Predictive methods such as Harrington's [24] are based on regression models derived from pelvis geometry; however, as humans differ anatomically these methods do not allow for patient customization leading to high variations. In an attempt to better these results, functional methods such as Gamage and Lasenby's [26] were developed. These methods rely on data obtained from skin markers positioned along a patient's pelvis and thigh regions. Assuming that the HJC is a ball and socket joint, trajectories of the markers are used to estimate the centre of rotation by having the patient carry out *ad hoc* motion of their leg. The main problem with this method is its inability to differentiate between the physiological movements of the skin

markers over the underlying bone due to muscle contraction and synchronous shifting from soft tissue artifacts (STA) [17]. Although functional methods have shown to produce more reliable results, due their to cost and complexity, predictive methods are still most widely used.

Despite the lack of accurate methods, not much advancements have been made in locating the HJC. The use of non-invasive devices such as ultrasound and MRI are favorable techniques that can be used for verification of the HJC. However, due to the cost and magnetic radiation associated with MRI [29], ultrasound verification looks very promising. Its non-ionizing and non-invasive nature makes it a great diagnostic medical device in locating the HJC.

## **1.2 Aims**

A previous study carried out by Romana in 2012 [40], underlined the potential benefits of using an ultrasound medical device for locating the HJC. The aim of her study was to identify the main causes of STAs and to determine their effects in the accuracy of using predictive and functional methods. For comparative purposes, ultrasound and MRI imaging were also looked into. However, only the prospect of using an ultrasound machine was investigated; its verification for locating the HJC was not studied.

Therefore, the aim of this project was to develop a technique that could be used to locate the hip joint from ultrasound imaging and to compare these results to the functional method proposed by Gamage and Lasenby [26], which have been identified as producing the most accurate results to date [27].

## **2 Literature Review**

### **2.1 Principles of Ultrasound**

Over the last decade, the use of ultrasound imaging, also known as sonography, has become increasingly popular due to its simplicity in operation and safety. Progressively ultrasounds have been used for monitoring other bodily tissues in clinical settings; apart from its primary intended function of visualizing fetal development, ultrasounds have been used for identifying a variety of medical conditions proving to be an excellent diagnostic tool [1].

Ultrasound imaging involves the positioning of a transducer or probe coupled with ultrasonic gel on a targeted region of the body to expose body tissues to high-frequency sound waves [2]. As ultrasound imaging is captured in real-time, tissue structures, internal organ movements and blood flow through vessels can be easily detected.

Currently there has been a huge drive in the use of ultrasound for visualizing the hip joint. Ultrasound imaging can be used to provide details of muscles, tendons, ligaments, and soft tissue of the hip joint. It is mainly used as a diagnostic technique to identify abnormalities in tissue structures such as tears, muscle fluid collections, soft tissue tumors, rheumatoid arthritis and developmental dysplasia of the hip (DDH). This technique is particularly carried out in infants where the hip is composed mainly of cartilage, producing clear and recognizable ultrasound imaging [3]. Table 2.1 summarizes the main benefits of using ultrasonic devices.

**Table 2.1:** Use of ultrasound medical device

<b>Benefits</b>	<b>Disadvantages</b>
Noninvasive	Temporary Subject Discomfort
Non-Ionizing Radiation	Subjective Image Analysis
Good Soft Tissue Imaging	-
Real-time Imaging	-

### **2.1.1 Characterisation of Ultrasound waves**

Image formations from ultrasonic devices are based on an energy source that is supplied externally to the object under examination in the form of continuous sound waves also known as pulses. The sound waves that are used in ultrasound machines are ranged above the acoustic frequency of 20kHz. For general medical imaging, a frequency of 2-18MHz is usually employed [3,7]. Such high frequencies are required, as they possess lower wavelengths compared to the objects that are being studied. This difference in wavelength across the interface allows the sounds waves to be reflected and refracted.

Although different modes of wave propagation are possible at ultrasonic frequencies, longitudinal waves are used in diagnostic ultrasound as they can be detected by biological tissues [4]. Unlike magnetic waves, sound waves require a medium to propagate and produce particle displacement. These waves propagate through the entire medium, vibrating the underlying particles. The transmitted or refracted wave then continues to travel along the direction of the propagation determined by the velocity of the medium.

### **2.1.2 Ultrasonic Parameters**

Ultrasound waves are characterized by the medium's physical parameters including density, temperature and viscosity [5].



The velocity of the sound wave propagation depends on both the elasticity (E) and the mean density ( $\rho$ ) of the medium, defined by  $v = \frac{\sqrt{E}}{\rho}$ . As ultrasounds are mainly used for imaging tissue structures, the velocity that is used for designing medical ultrasonic equipment is approximately  $1.54 \times 10^3 \text{ ms}^{-1}$  which coincides with the average velocity of soft tissue [5].

Acoustic impedance (Z) is defined as  $\frac{P}{V}$ , where P is the acoustic pressure created by the compression and expansion of the acoustic waves and V is the local particle velocity created by the displacement of the vibrating particles at a given instance in time [6]. Acoustic impedance causes the sound waves to be reflected at various degrees due to differences in surface impedances. This variation in the degree of reflection of the ultrasound waves allow for multiple surface detection [5,6]. The Table 2.1.2 lists the velocities and impedances of different media.

**Table 2.1.2: Ultrasound Velocities and Impedances [6]**

<b>Medium</b>	<b>Velocity (<math>10^3 \text{ ms}^{-1}</math>)</b>	<b>Acoustic Impedance (<math>10^6 \text{ kg m}^{-2} \text{ s}^{-1}</math>)</b>
Air	0.331	$0.4 \times 10^{-3}$
Blood	1.57	1.66
Bone	2.5-4.7	4.0-7.5
Brain	1.54	1.66
Fat	1.45	1.33
Kidney	1.56	1.62
Liver	1.57	1.66
Muscle	1.59	1.70
Distilled water	1.54	1.48
Ultrasonic Gel (Propylene Glycol)	0.13	1.61

The main challenge of using ultrasonic devices is visualizing the targeted structures with strong signals. The further the acoustic waves travel, especially incases where deeper

structure are required to be imaged, the more the sound waves are attenuated, reducing their signal strength i.e. echo amplitude. Attenuation is mostly caused by the propagation of the waves through inhomogeneous substances such as tissue. As attenuation is linearly proportional to frequency, higher frequencies lead to limited degrees of penetration. Therefore, the swept gain or time-gain compensation function on ultrasound devices are used to amplify the signal strength from deeper structures [3, 6].

### **2.1.3 Detection of Ultrasound**

Transducers, also known as probes, are used to generate and transmit ultrasonic waves through the use of piezoelectric properties. These transducers are built using multiple layers. The first or front layer is matched to the impedance of tissue to allow for good energy transfer. If the matching is poor the energy transferred would decrease, causing ringing artifacts. Crystals such as polyvinyl fluoride, barium and quartz [5,7] are mainly used as the matching material as they have similar impedance to both the tissue and the middle layer of the transducer.

The middle layer is constructed from a piezoelectric material. These specialized materials vibrate based on their thickness at different resonant frequencies. This gives the material the ability to convert between electrical and acoustical energies. Piezoceramics, such as lead zirconate titanate (PZT) are most commonly used in transducers [7,8,9]; however, new composite materials such as lithium niobate, are also being employed for high performance 2D array transducers. The simplest forms of transducers consist of a single piezoelectric disc or element [7].

A damping block or backing material is then positioned directly behind the piezoelectric element [8] to absorb and damp some energy from the crystal to reduce the duration of the pulse i.e. shorten the pulse time, Figure 2.1.3A.

***Figure 2.1.3A: Transducer (Probe) design of an ultrasound [Modified from 8]***

A conductor is used to coat the surface of the matching layer so that when a voltage from an external source is applied, the piezoelectric material can deform by thickening. The amount of deformation or strain of the piezoelectric material depends on the voltage applied. An alternating voltage which is used in mains, causes an alternating strain with a frequency equal to that of the voltage applied. Therefore, an ultrasonic wave of the same frequency is emitted [6,8].

Various types of arrays can be transmitted from transducers to produce different types of scans. The two most commonly used include the linear array, where pulses are transmitted separately producing a well-defined beam, and the convex array, where pulses are transmitted simultaneously producing a larger field view [9]. However, the creation of a larger field view is compromised by poorer resolution at the ends of the transducer, Figure 2.1.3B.

**Figure 2.1.3B:** Ultrasound Transducer Array: (a) Linear (b) Convex [Modified from 9]

Ultrasound scanners use these transducers to steer the ultrasound beam to generate fast imaging, usually within milliseconds. A diagram of the steps involved in generating an ultrasound image is provided in Figure 2.1.3C.

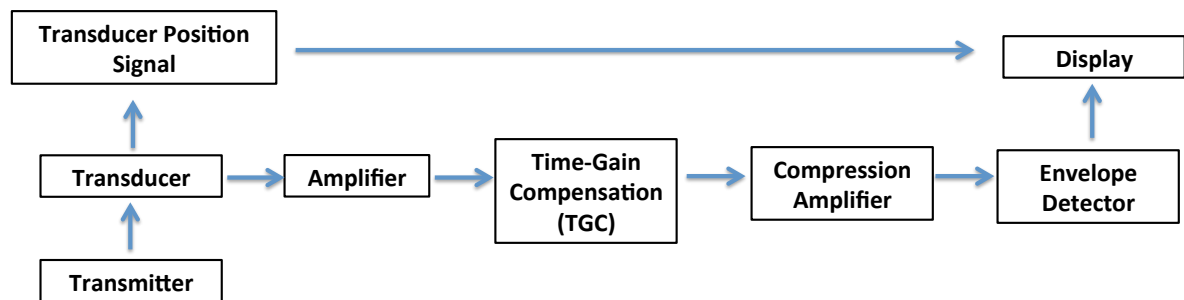


**Figure 2.1.3C:** Flow diagram of the generalized steps of an Ultrasound device

## 2.1.4 Imaging Methods

Ultrasound images are constructed from returned and transmitted waves. There are two basic types of imaging methods: the Pulse-Echo system and the Doppler system. Each of these procedures involve different scan modes for generating images [10].

### 2.1.4.1 The Pulse-Echo System

The Pulse-Echo system images the reflected energy incidents that are transmitted to the patient. The signals are amplified using the time-grain compensation. This method uses three main types of scanners.

***(i) A-mode Scanner***

The amplitude mode (A-mode) scanner is an oscilloscope type scanner in which the echo amplitude is plotted against the distance travelled by the wave. This method relies on the reflected signal to build up an image rather than on the actual underlying structural image. The main downfall to this scanner is its sensitivity to error as it relies on the angling of the probe.

***(ii) B-mode Scanner***

The brightness mode (B-mode) scanner is composed from a collection of A-mode intensity lines. The intensity of the echoes are based on the position and depth of the structure being studied. Images are generated by displaying the intensity of the amplitude of the echoes.

***(iii) M-mode Scanner***

The motion mode (M-mode) scanner fixes the transducer in a single position to display the A-mode intensity lines as a function of time. Images are built by following the movement of the echoes over time.

**2.1.4.2 The Doppler System**

The Doppler system allows for real time motion detection and imaging by moving a reflector between the source and the transducer. There are five different types of Doppler systems.

***(i) Continuous Wave (CW) Doppler***

The Continuous Wave (CW) Doppler emits sinusoidal ultrasonic waves. The echoes that are reflected are amplified and a demodulator is used to calculate the frequency between

the transmitted and reflected waves. The difference between these frequencies is then displayed as the output image.

***(ii) Pulsed Doppler***

The Pulsed Doppler emits short pulses at regular intervals to the underlying structure. The time delay between the transmitted and reflected waves are calculated so that signals only from a selected range or depth interval are detected and imaged. Unlike the CW Doppler they have a range gate or a fixed sample volume.

***(iii, iv) Colour and Power Doppler***

The Colour and Power Doppler both use the B-Mode scanner and impose either a colourized map to indicate the intensity of flow or combine a steerable Doppler beam allowing simultaneous display of the Doppler spectrum.

***(v) Tissue Doppler***

The Tissue Doppler combines the power Doppler with a low pass filter to remove low frequencies to enable wall motion detection for blood vessels imaging.

## **2.2 Hip joint centre**

### **2.2.1 Significance of The Hip Joint Centre**

The location of the Hip Joint Centre (HJC) is important for accurately determining both the kinematic and kinetic data during studies of human motion. The location of the centre of rotation of various lower limb joints, including the HJC, should be located as precisely as possible for proper gait analyses. Current methods used till this day have not been so successful.

The location of the hip joint centre has been estimated either using functional or predictive methods, refer to Section 2.3 for details. Through various studies, functional approaches have been recommended due to their higher precision [11]. However these methods require specific algorithms in which patients are required to carrying out *ad hoc* movement using their hip and leg. A study carried out by Stagni *et al* in 2000 [17], showed the effects of inaccurately locating the hip joint. It was reported that both the ankle and hip moments were affected causing large propagation errors mainly in the flexion-extension direction.

### **2.2.2 Anatomy and Axis System**

The hip joint is situated in the pelvis usually described and represented as a ball and socket joint, Figure 2.2.2A. It is symmetrical with bony projections of concave and convex areas with the acetabulum accommodating the femoral head. A pad of fibrocartilage surrounds the surface of the bone reducing friction and allowing easy joint movement for flexion, extension, adduction, abduction, circumduction and rotation. The bony socket, supporting ligaments and muscular padding makes the hip joint very stable [12].

**a**

**b**

**Figure 2.2.2A:** Hip anatomy: (a) Anatomical model of the hip; (b) Ball and Socket model of the hip [Modified from 13]

The axis system used till this date is based on the conventional system developed in 1993 by the Standardization and Terminology Committee (STC). The Joint Coordinate System (JCS) developed by Grood and Suntay [14] is used as the standard for reporting joint motion for biomechanical calculations, making it easier for interpretation by clinicians. The JCS uses the Cartesian Coordinate System (CCS) to define two adjacent bony landmarks that are palpable or that can be easily pointed out using an X-ray device.

Establishing a JCS for the hip joint is more difficult than that of the ankle or knee as its landmarks are not that simple to access in practice. The hip joint is treated as a ball and socket joint with its centre of rotation being equated to the centre of the hip joint for biomechanical research [15].

The most common axis system used for locating the HJC is based on the model suggested by Wu et al in 2002 [16]. This model combines two axis systems. The first axis uses the HJC as the origin for the pelvis and femur head, the second axis relates the midpoint of the two femoral epicondyles by using the HJC to locate the proximal and distal axis. Markers are conventionally positioned on the bony landmarks of the pelvis: Anterior Superior Iliac Spine (ASIS), Posterior Superior Iliac Spine (PSIS) and Femoral Epicondyle (FE)  
Figure2.2.2B.



*Figure 2.2.2B: Axis system for the Hip and Femur [16]*

### **2.2.3 Challenges in Locating the HJC**

Regardless of the axis system used, a series of markers have to be positioned on the pelvis and thigh regions of the body to identify and locate the HJC. However, the accuracy of identifying the HJC is affected by a series of factors including instrumentational errors, incorrect marker cluster geometry, poor algorithms, and most crucially movement due to skin markers. As the markers cannot be directly positioned on the underlying bone, the skin layer causes these markers to slightly move; this phenomenon is referred to as Soft Tissue Artefact (STA).

Over the years, a series of studies have been conducted to help reduce the errors associated with STA in locating the HJC. Stagni *et al* [17] were able to reconstruct 3D kinematics of the femur and tibia from fluoroscopic images taken from two patients with above knee prosthesis to quantify STAs around the thigh and shank. Their findings suggested that STAs mainly affected the abduction and adduction of the knee joint. It was also reported that the STAs accounted for a 31mm displacement on the thigh and a 21mm displacement along the medial-lateral direction of the shank. This study showed that external markers could only be used for flexion and extension calculations at the knee joint and not for

adduction and abduction due to the presence of STA, incorporating a root mean square error of 117% and 192% respectively.

However, recently in 2012, two different techniques were explored in an attempt to reduce STAs. One of the techniques involved identifying optimal regions of the thigh for skin marker location; the other technique involved the development of a mathematical model to predict STAs.

The first technique was investigated by Krutzenstein *et al* in April 2012 [18]. Their study involved placing sixty-three retro reflective skin markers on the thigh and an additional sixteen markers on the pelvis of seven healthy subjects. In order to identify the markers that had the biggest impact on locating the centre of rotation (CoR) of the hip, the Weight Optimal Common Shape Technique (wOCST) was employed. This technique assigns different weights to each marker to allow the identification of the markers that have the highest contribution to the determination of the CoR. This approach has recently gained popularity due to its high precision for determining joint centres *in vivo* by incorporating non-uniform STA distribution.

From the sixty-three markers used, six areas of highest importance were identified by averaging the weightings from each marker for all subjects. These regions were verified by comparing their residual values to that of all the sixty-three markers used. The mean residual ( $r$ ) for all the markers ( $2.7 \pm 0.5 \text{mm}$ ) was comparable to the six markers positioned on the optimal areas ( $3.6 \pm 0.6 \text{mm}$ ). This demonstrated that the effective placements of only six markers on the thigh region could produce similar results to that of a redundant set of sixty-three markers.

These effective areas identified are located away from the joint itself, reducing STA and increasing the signal to noise ratio for locating the HJC, Figure 2.2.3A. These six areas included the proximal and distal areas of each of the anterior, posterior and lateral surfaces of the thigh, Table 2.2.3A summarizes these identified regions.

*Figure 2.2.3A: Optimal regions for marker placement [Modified from 18]*

*Table 2.2.3A: Summary of the optimal regions for marker placement*

<b>Region</b>	<b>Marker</b>	<b>Area</b>
1	Anterior marker 1 (AI)	Proximal from the belly of the Rectus Femoris
2	Anterior marker 2 (AII)	Anterolateral area of the distal thigh
3	Lateral marker 1 (LI)	Proximal along the tensor fasciae latae
4	Lateral marker 2 (LII)	Distal along the tensor fasciae latae
5	Posterior marker 1 (PI)	Proximal from the belly of the Biceps Femoris
6	Posterior marker 2 (PII)	Distal of the belly of the Biceps Femoris

However, it should be noted that this study's assessment of the residuals was based on the CoR and not on the location of the HJC itself. Although the hip joint can be considered as a sphere and so the range of hip motion in determining the CoR could help locate the HJC, it does not provide a direct means of correcting STA for locating the HJC.

The second technique was recently explored by Comomilla et al in September 2012 [19]. Their study involved modeling and building up a realization of STA by selecting twelve regions of the thigh, Figure 2.2.3B. Table 2.2.3B summarizes the marker positions.

**Figure 2.2.3B:** Position of the markers along the thigh and pelvis region [19]

**Table 2.2.3B:** Number of markers and their respective positions

Skin markers	Position
4	Antero-Lateral(L)
4	Antero-Medial(M)
4	Anterior (A)
Calibration markers	Position
1	Right Anterior Superior Iliac Spines (RASI)
1	Left Anterior Superior Iliac Spines (LASI)
1	Right Posterior Superior Spines (RPSI)
1	Left Posterior Superior Spines (LPSI)
1	Lateral Femoral Epicondyles (LE)
1	Medial Femoral Epicondyles (ME)

The STA was predicted and modeled using a cost function based on the difference between the root mean square of the measured and estimated STA components:

$$f(h_{s,t,k,c}) = \sqrt{\frac{1}{N} \sum_{j=1}^N [a_{s,t,k,c,j} - \tilde{a}_{s,t,k,c,j}(\alpha_j, \beta_j, \gamma_j)]^2} \quad r_{s,t,k,c} > 0 \quad (2.2.3)$$

Where:  $a_{s,t,k,c,j}$ : Measured STA

$\tilde{a}_{s,t,k,c,j}$ : Estimated STA

$\alpha_j, \beta_j, \gamma_j$ : Hip Joint Angles (flexion-extension, abduction-adduction, internal-external rotation respectively)

N: Number of trials

The cost function equation developed was able to remove the error associated with STA displacement, confirming that STA realization is plausible using mathematical manipulations. This study also showed the importance of markers location; the markers located along the antero-medial (M) longitudinal lines were most susceptible to STA with an average displacement of 22mm compared to the anterior-lateral (L) with an average of displacement of 10mm.

However, the main limitation with this study was based on their assumption of zero knee movement, this omitted the STAs that were caused by the rotation of the knee. In addition, skin stretching was the only STA artifact that was looked into, other factors such as wobbling of the soft tissue masses caused by muscle contraction of the gluteal region was not investigated. Therefore, the accuracy of their report is highly subject-dependent; reference to the same data could produce different results due to differences in human anatomical geometries.

### **2.3 Current Methods**

There are three techniques that are currently being used for locating the HJC. These techniques are divided into predictive, functional and validation methods.

#### **2.3.1 Predictive Methods**

Predictive methods used to locate the HJC are based on regression equations developed from the pelvic width and geometry. Since the 1980's three main regression equations have been widely used in locating the HJC. These predictive models include Bell's, Davis' and Seidel's regression equations [20, 21, 22].

Extensive comparative studies have been carried out to compare the different predictive methods available in an attempt to identify the most accurate. The first study was carried out in 1999 by Leardini *et al* [23] where they compared Bell's, Davis' and Seidel's regression equations with the "true" HJC using Roentgen Stereophotogrammatic Analysis (RSA). From these findings, Bell's method proved to be the least accurate as it relied only on pelvic geometry excluding the patient's leg length. This caused a low correlation factor of the pelvic width in both the x and y coordinates: 0.21 and 0.24 respectively. Seidel's model, on the other hand, was identified as the most accurate as it incorporated the patient's leg length. However, it was determined as impractical due to the awkward pubic landmarks that were used for the regression equations.

The most recent comparative study was carried out in 2007 by Harrington *et al* [24]. Their study involved the use of MRI imaging for validation. They too obtained similar results as Leardini *et al* [23]; however, apart from locating the HJC they also focused on locating the ASIS and PSIS landmarks. This allowed them to develop their own set of pelvis-embedded coordinate system derived from the axis system developed by Wu *et al* [16] as described in Section 2.2.2. These equations are most widely used for locating the HJC in clinical settings to date.

### **2.3.2 Functional Methods**

In an attempt to improve predictive methods, functional methods, also known as sphere-fitting models, were developed to allow for individual customization, reducing error. These models are based on the principle that the HJC is a simple ball and socket pivot joint, where the thigh moves in relation to the pelvis forming vectors which are used to create concentric spheres. Although, it has been slow to gain popularity due to the high cost in equipment

and software that are required, it has been continuously modified to produce more accurate results.. This idea was first proposed by Aurelio Cappozzo in 1984 [25]. Over the years, his method has been modified and improved to assist in locating the HJC.

The most widely used functional method to date was developed in 2002 by Gamage and Lasenby [26]. Comparative studies carried out by various groups including Rainald Ehrig *et al* [27] have identified this method as the most accurate. Gamage and Lasenby regression equations rely on the use of skin markers. This method is based on the idea that vectors produced by the hip joint move with a fixed centre of rotation around an axis producing spherical trajectories. This allows for the centre of rotation to be calculated without the need for averaging the data obtained from the markers, reducing error. It should be noted that this method is not free from bias. The error associated with locating the HJC was assumed to be directly related to STA; however, upon further investigation no direct relationship has yet been identified between the magnitude of the STAs and the displacement error in locating the HJC.

### **2.3.3 Validation Methods**

The use of either predictive or functional methods in locating the HJC are highly time consuming and inaccurate. The use of alternatives such as medical equipment that allow visualization inside the body can be used to eliminate the need for skin markers. Apart from the use of ultrasounds, X-ray and MRI devices are other two commonly used imaging techniques.

### **2.3.3.1 X-Rays**

X-rays emit high-energy radiation with short wavelengths that can penetrate bodily tissue easily. As the body is composed of organs and tissues with various densities, different amounts of radiation are penetrated across various structures. As bone is the densest component in the body, the x-rays cannot pass these highly structured calcium hydroxyapatite layers and are instead reflected. A film is placed between the subject and the x-ray beam to make up the image of the reflected rays. X-ray validation of the HJC was first used by Bell *et al* [21] in 1990 as it was considered to be the gold standard for medical diagnostics. However, due to the carcinogenic effects of x-ray radiation, many researchers have stopped using this technique [28].

### **2.3.3.2 Magnetic Resonance Imaging**

Magnetic Resonance Imaging (MRI) use a magnetic field to line up protons found in hydrogen atoms that build up water molecules inside the human body. Radio waves are used to excite these hydrogen atoms moving them into a higher energy state. Once the source of emission of the radio waves is removed, the hydrogen atoms move back down to their natural energy states releasing energy. This released energy is then detected by a scanner and an image is created. An MRI image is composed of multiple slices taken from one session. These slices allow for the creation of 3D images [29].

Apart from being used as a diagnostic device, MRI machines have been recently used as a validation technique in determining the HJC. Harrington *et al* [24] were one of the first groups to use MRI as a validation technique for locating the HJC. Heller *et al* [39] shortly followed and used MRI to model 3D images of the knee joint to examine and validate new knee kinematic models.



The underlying issue with using MRI is their cost and availability. The ability to conduct research using MRI is extremely difficult due to the limited number of these devices that are available per hospitals and clinics.

### **2.3.3.3 Ultrasound**

Ultrasounds like X-ray machines rely on tissue density to form images as described in Section 2.1. As ultrasounds are non-invasive and are relatively inexpensive to operate, they have gained popularity in clinical settings. Traditionally they have been used to image and monitor soft tissue, including developing fetuses, heart function, blood flow and organ related cancers [30,31]. Using ultrasound for imaging bone is highly challenging due to their high impedance [32].

However in 2005, Hicks *et al* [33] were the first to use an ultrasound to validate their sphere-fitting ball and socket model for locating the HJC. A linear probe with a frequency of 10MHz was used to obtain images from the frontal horizontal and vertical positions of the femoral head. Their findings suggested that the use of ultrasounds for locating the HJC was not accurate as the interpretation of the images were highly subjective. Using a highly experienced individual with complete knowledge of the human anatomy could be beneficial; however, if ultrasounds are to be used for bone-imaging improvements must be developed.

## **2.4 Current Ultrasound techniques for locating the HJC**

The main challenge of using an ultrasound for verifying the HJC is its subjective image interpretation. A series of studies over the last few years have either tried to develop new procedures that allow for quantitative image analysis of bones at various skeletal sites or

have tried to develop techniques that can convert 2D ultrasound images into 3D, allowing spatial studies for accurately locating joints.

The first successful study using ultrasound verification was carried out by Peters *et al* in 2010 [34]. Their study showed that the use of 3D-ultrasound (3-DUS) could provide an excellent validation technique for locating the HJC. As part of their study, 3-DUS images were created from 2-DUS by placing three reflective markers on a triangular shaped phantom attached to an ultrasound probe, Figure 2.4A.

***Figure 2.4A: 3D-US Probe with markers attached in a triangular configuration [Modified from 34]***

The movements of these markers were detected by a motion analysis system. The system was calibrated using the Cambridge stylus method. This calibration technique was proved to be the most effective by an earlier study carried out by Hsu *et al* [35] at the University of Cambridge. The Cambridge stylus phantom is specifically designed to produce lines in the B-Scan of an ultrasound; whereas, other currently available calibration techniques such as the sharp, spherical and rod styluses are all based on a point phantom design. These methods require precise alignment with the ultrasound scan, leading to longer processing times and poorer image resolution, Figure 2.4B.

**Figure 2.4B:** *Ultrasound images obtained from different calibration styluses: (a) Sharp (b) Spherical (c) Rod (d) Cambridge [Modified from 35]*

In addition, Peters *et al* carried out a direct comparisons between the results they obtained from the 3-DUS to MRI imaging using the least squared fitting technique developed by Gamage and Lasenby. Their study showed that both methods had the ability to produce similar results with a mean difference of  $4 \pm 2$ mm. However, despite this optimistic study, the authors fail to provide sufficient details regarding their methodology. Further inquiries and investigations should be carried out to verify their results and confirm consistency in the data they obtained using the 3DUS.

In 2012, Sangeux *et al* [36] conducted another comparative study using an ultrasound on 53 children with cerebral palsy. This study looked into the accuracy of using predictive and functional methods against the 3D ultrasound (3-DUS) technique developed earlier by Peter *et al*, mentioned above. The predictive methods investigated included Harrington's and Davis's models and the functional methods included a global calibration method, two sphere fitting methods (geometric and algebraic) and two transformational methods (Centre Transformation Technique (CTT)) and Symmetrical Centre of rotation Estimation (SCoRE)).

From this study it was concluded that Davis's regression equations gave the poorest results with the most displacement discrepancies compared to the data obtained from the 3DUS. The functional methods also did not prove too accurate, as the disabled subjects had limited

range of movement, increasing error in the anterior and posterior directions. Harrington's equation, on the other hand, produced the most accurate results with 80% of the hip locations of the 53 subjects falling between 20mm from the ultrasound measurements. Although, these findings are not too promising, as a 20mm difference would have a huge impact on gait analysis, this study has shown that the use of 3-DUS can be used as a validation technique, and can be used with both functional and predictive methods that are currently being used in clinical settings providing a corrective step for predicting the HJC.

Other recent studies have looked into signal processing techniques for enhancing ultrasonic images obtained from bones. Lasaygues *et al* [37] have looked into the use of tomographic ultrasonic procedures for determining the local velocity of long bones more precisely in an attempt to generate higher image resolution. The main challenge of using tomographic procedures for bones is their high contrast in acoustic properties between soft tissues. They devised an algorithm for tomographic compensation image processing where they included a summation of all the projected filters they used: measurement, computation and spreading. Their algorithm allowed for sound velocity compensation of the images using *a priori* knowledge. Their compensation procedure was modified to correct for the hollow part of bones. This was done by considering the bone as a multi-layer medium dividing both the parallel and plane interfaces into zones, Figure 2.4C.

**Figure 2.4C:** *Compensation Correction Procedure [37]*

The use of the compensation reconstruction procedure produced improved ultrasonic images of the femur. Using the newly set velocity of  $2400\pm 400\text{ms}^{-1}$ , identified by the compensation reconstruction procedure, produced better image contrast and reduced the blurring effects that were present in the images using the standard mean sound velocity of  $2500\pm 700\text{ms}^{-1}$  without applying the reconstruction procedure, Figure 2.4D.

**Figure 2.4D:** *Cross-section of the human femur (a) without (b) with the compensation reconstruction procedure [37]*

Methods for reducing subjective ultrasound image interoperations have also been investigated by developing codes to generate 3D ultrasound imaging. In 2011, Honk Kong Polytechnique University [38] focused on converting 2D ultrasonic images into 3D in real time, using MATLAB. The advantage of using such programming techniques is that it allows image control using hybrid segmentation to produce highly detailed 3D reconstructions removing the need for subjective image analyses. Results from this study, showed that the measured volume error of the multi-view reconstruction was less than 5% of the true volume.

These studies have shown that the use of ultrasounds in locating the HJC is feasible and quite accurate; further verifications of these findings can make ultrasounds the new gold standard for locating the HJC.

### **3 Methodology**

#### **3.1 Background**

A method that accurately locates the HJC has still not been developed. The first methods developed, known as predictive methods, were derived from patient's anatomical geometry and on the assumption of perfect symmetry of the pelvis. The differences in anatomical geometry between subjects and the unrealistic assumption of perfect symmetry, especially in cases where subjects suffer from pelvic deformities, make these methods unreliable. The use functional methods such as the ones based on Gamage and Lasenby use sphere-fitting models that have proved to produce more accurate results despite their incorporation of STAs.

Using validation techniques such as ultrasound to locate the HJC can produce highly accurate results without the need for prolonged experimental times and complicated procedures as described in Section 2.4. However, there is still not a standardized method for using ultrasound devices for locating the HJC.

This study will assess the use of ultrasound imaging for locating the HJC. The accuracy of using ultrasound devices will be compared to Gamage and Lasenby's functional method for verification in an attempt to identify the method that has the most potential for producing reliable results.

### **3.2 Subject Testing**

A 25 year old female subject, with a height of 166cm and a weight of 56 Kg, volunteered to participate in this study. The subject was a healthy member of the university and provided informed consent in accordance with the University of Strathclyde's code of ethics and guidelines, refer to Appendix A. Subjects whose Body Mass Index (BMI) was not in the range of 18-25 were excluded from the study in an attempt to not only minimize errors associated with STA but to also allow for more accurate ultrasound imaging.

### **3.3 Phantom and Tissue Mimicking Model**

A 50cm rigid polyurethane plastic femur model manufactured by Sawbones Inc. was used as a phantom to practice imaging using various ultrasonic techniques. This particular model was used as it was directly available from the Biomechanic's Laboratory. The main benefit of using such a model was that it also allowed for ultrasound imaging using different coupling media; this study particularly looked into the use of ultrasonic gel and water for generating ultrasonic scans.

The femur model was imaged under water using two methods, Figure 3.3A. The first simply involved submerging the head of the free femur model into a 20cm x 12cm clear low-density polyethylene container. The ultrasound transducer was then held in position and the model was rotated so that the complete femur head and start of the femoral shaft could be imaged. The second method involved using a fixed femur model held in position with two screws along its length in a clear 25cm x 60cm Perspex rectangular plastic container. This time, as the model was fixed, the transducer was made to go around the femoral head and shaft.

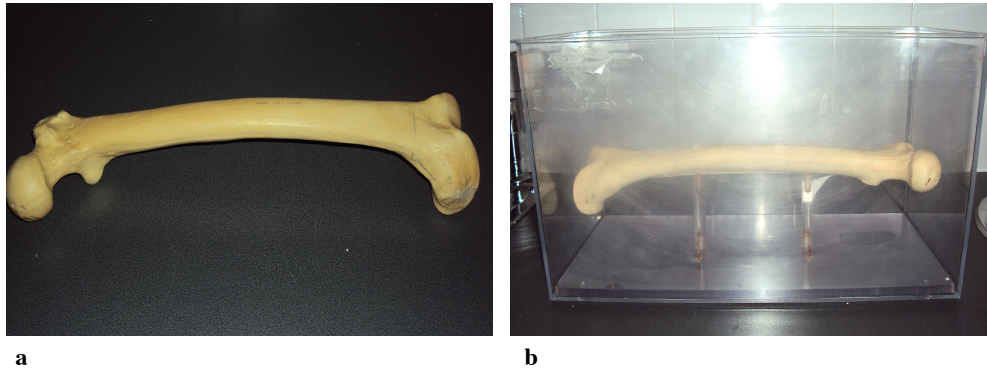


**Figure 3.3A:** *Femur Model (a) Unfixed model (b) Fixed model*

To create a medium that was similar in nature to tissue, a wheat flour (*Triticum Vulgare*) based adhesive, commonly applied for wallpaper paste, was used to create a solution in which the femur model was submerged. To prepare this tissue mimicking medium, 50grams of the wheat based adhesive was mixed with 0.5liters of cold water at room temperature in a clear 20cm x12cm polyethylene container and was set for thirty minutes. This produced an opaque high viscous media, Figure 3.3B.



**Figure 3.3B:** *Tissue Mimicking material made from wheat flour adhesive*

### **3.4 Ultrasound Imaging**

The Toshiba SSA-325A Ultrasound was used to obtain ultrasound images of both the phantom model and subject. This machine allowed for both M and B mode scanning, it also contained two ports which allowed for the connection of two separate transducers simultaneously. The main challenge of using this device was its date of manufacture (2002). It lacked many of the data processing kits that allow for clear and sharp image formation. Another downfall of the Toshiba SSA-325A Ultrasound was that it did not have



the capability of converting and storing digitalized data. A video capture USB cable from StarTech was used to transfer the analogue ultrasound signal into digital format and to record videos and capture pictures as .MPEG and .JPEG files respectively.

In an attempt to verify and obtain better images, two newly designed and manufactured ultrasound devices currently being used in hospitals and clinical settings were tested; these included the Zonare z.one and the Ultrasonix Tablet. The Zonare z.one Ultrasound is unique in that it acquires and implements the data acquisition in a software rather than hardware, reducing the size and weight of the ultrasound machine. It also allows for faster imaging, reducing motion artifacts in images. The Ultrasonix Tablet is a compact and portable ultrasound system with a touch screen. It has a built in recorder that allows for up to sixty minutes of video capturing in .MPEG format. It also supports multiple image modes, from the basic B and M mode to the Pulsed, Continuous and Colour Flow wave Doppler; it also offers Trapezoidal and Panoramic Imaging.

### **3.5 Mimics Software**

To obtain a local coordinate axis and to determine the radius of the femoral head from the ultrasound images obtained, the Mimics 12.01 software developed by Materialise was used. This software has been specifically designed for medical image processing. It enables segmentation of 2D images to produce 3D models. It is currently used as a gold standard for generating 3D models of patient's anatomy using CT and MRI scans. Although not much studies have been carried out using Mimics for ultrasound image processing, this project attempted to generate these 3D models for detailing the hip joint and geometry for determining the HJC location.

### **3.6 Experimental Design for Ultrasound Imaging**

As bones reflect ultrasound waves, their underlying surfaces appear as bright lines. Accordingly, the gain-compensation for all trials were kept under 40% for consistency in an attempt to obtain better ultrasound bone scans. Although reducing the gain-compensation produce poorer image quality, as the attenuated signals are prevented from being amplified, in the case of this experimental study high image quality for detailing fine vessels or tissue structures were not necessary as the aim of this project was to simply locate the HJC.

Two different tests were proposed using the Toshiba SSA-325A Ultrasound. The first test was designed to obtain ultrasound images from both the phantom model and the subject using a transducer matched with a coupling media. The second test was designed to obtain coordinates from the ultrasound transducer relative to the bony landmarks of the pelvis. For both tests, a narrow array was specifically chosen for the transducer. With a smaller field view direct imaging of the targeted structure was possible. Therefore, the position of the probe could roughly indicate externally on the body the location of the hip joint.

For the second test three reflective markers were placed on the linear probe using double-sided sticky tape. These markers were positioned in a triangular setting in order to create a plane, Figure 3.6a. The probe was first used to mark the area of the subject's hip joint area determined by the live images obtained from the Toshiba SSA- 325A. The probe was then positioned on the marked area of the skin and was held in place to obtain static data from the Vicon motion system, Figure 3.6b.

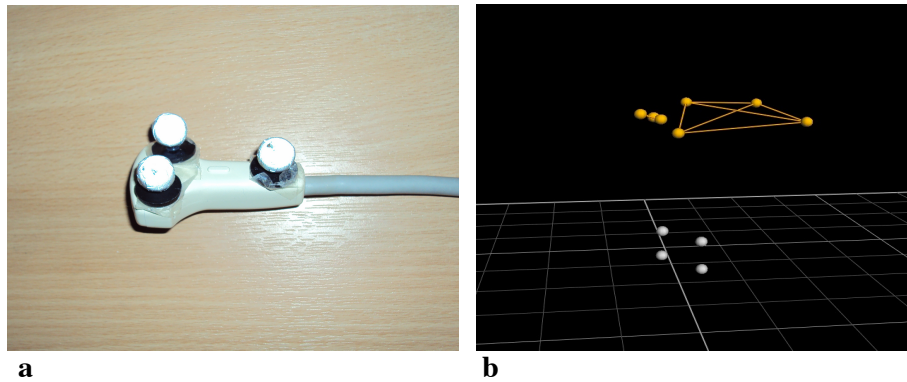


**Figure 3.6:** Use of the Ultrasound Probe with the Vicon Motion Capture System (a) Reflective markers located on the probe; (b) Screenshot of the reflective markers placed on the probe and pelvis region

### 3.7 Functional Method verification

As discussed in Section 2.3.2, the preferred method for verification is based on Gamage and Lasenby's regression equations. This method relies on the trajectories of individual reflective markers placed along the subject's hip and thigh. The circumduction of the leg allows the construction of vectors from the axis of rotation, forming tips from concentric spheres. A least square equation is then applied between the distance of each marker to calculate the HJC. Therefore, the functional method based on Gamage and Lasenby was used in this study for verifying the location of the hip joint.

### 3.8 Motion Capture System

The Vicon motion capture system was used for collecting data from the reflective markers placed on the subject pelvis region based on Wu's axis coordinate system, refer to Section 2.2.2. Motion capture systems are used for not only motion tracking but also for analyzing moving body parts. Gait analyses allow the determination of both kinetic and kinematic parameters. These parameters can then be used as a diagnostic tool to treat patients suffering from various musculoskeletal disorders.

The Vicon motion capture system consisted of twelve infrared (IR) cameras placed around the Biomedical Engineering Gait Laboratory, Figure 3.8a. These IR cameras captured both the light and the position of the reflective markers in 2D plane views. The data obtained from all twelve cameras were combined to create 3D spatial imaging. The Nexus software was used to record and label each marker's position with time.

Before any testing, the Vicon motion capture system was calibrated both dynamically and statically. For the dynamic calibration, a calibration wand with 5 reflective markers was waved around the laboratory to activate the IR cameras. Once the twelve IR cameras were calibrated, the calibration wand was placed in the centre of the lab to build a global coordinate system for the static calibration. A frequency rate of 100Hz was used to record the coordinates of the individual reflective markers.

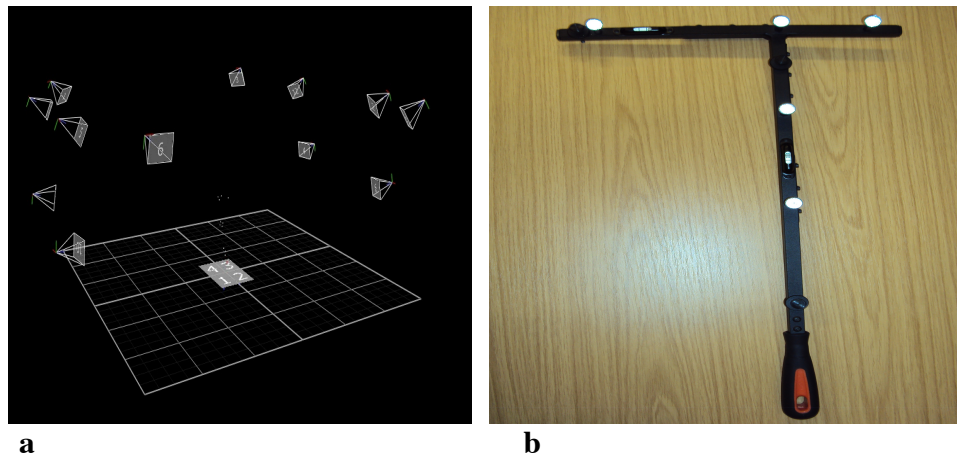


**Figure 3.8:** Vicon Motion Capture System (a) IR camera layout; (b) Calibration Wand

### 3.9 MATLAB Software

To process the data collected from the Vicon motion capture system, A MATLAB code based on Gamage and Lasenby's regression equations developed by Dr. Davydov and used by Romana in 2012 [40] was also used in this study for the functional verification method.

The MATLAB algorithm is based on the retro-reflective markers placed on the subject's hip and thigh to create both a global and local coordinate system. The trajectories of the markers from the thigh are transformed into a new defined axis system allowing the determination of these markers in relation to the HJC. From these new coordinates, the program can then determine the average centre of rotation common to all markers. The program can also estimate uncertainty by calculating the bias in relation to an ideal concentric sphere; refer to the Appendix B for the MATLAB code.

### 3.10 Experimental Design for the Vicon Motion Capture System

To determine a local coordinate system, the axis system proposed by Wu *et al* was adapted. This axis system has shown to provide good results with minimal STA effects. The positioning of the reflective markers on the subject was adjusted from Simpson (2011) [41]. A total of eight markers were used, Table 3.10.

**Table 3.10:** Positions of the 8 reflective markers on the Subject's thigh and hip area

Number of Markers	Position of Marker
1	Right Anterior Superior Iliac Spine (RASIS)
1	Left Anterior Superior Iliac Spine (LASIS)
1	Right Posterior Superior Iliac Spine (RPSIS)
1	Left Posterior Superior Iliac Spine (LPSIS)
2	Lateral along thigh
2	Anterior along thigh
Total: 8 Markers	

In an attempt to reduce the effects of STA to obtain more accurate results, two separate testing were carried out. The first set of tests involved placing the markers directly on the subjects skin using double-sided tape. The second series of tests involved positioning the markers on a cotton band wrapped around the subject's waist and thigh. This ensured that the markers were not directly placed on the subject's skin. This test was designed to determine whether placing the makers indirectly would reduce their movement caused by

skin stretching and muscle contraction along the thigh region reducing errors associated with STAs.

With the markers attached, the subject was then positioned in the centre of the laboratory and static calibration was conducted to record the local coordinate system Figure 3.10. After calibration, the trajectories from the eight reflective markers during the circumduction of the subject's right leg were captured by the Vicon system. A total of 14 trials were taken with each trial containing ten complete circumduction of the subject's right leg.

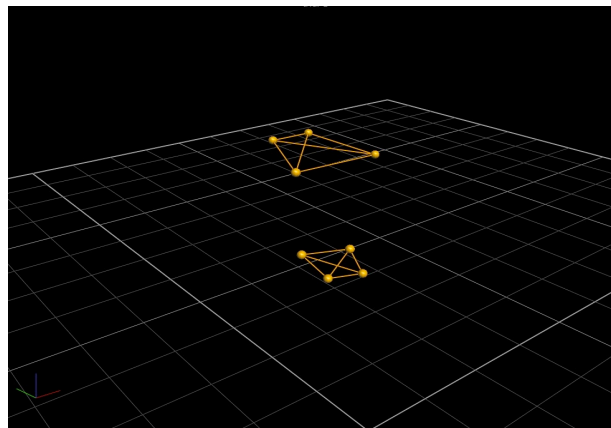


*Figure 3.10: Nexus Screenshot of the 8 markers located on the subject's pelvis and thigh*

### **3.11 Data Acquisition**

The videos and pictures captured by the Toshiba SSA-325A were saved as .MPEG and .JPEG formats respectively. For the purpose of using the Mimics software, describe in section 3.5, the images were converted into Bitmap (BMP) file format to allow for their importation. The MPEG videos captured were opened using the VLC Media Player and each video was converted to over 30 image slices. These image slices were then saved as BMP file format. The images obtained from the Zonare z.one and the Ultrasonix tablet were saved as DICOM format.

The data obtained by the Nexus program using the Vicon capture system described in Section 3.8 was saved as .csv files. This allowed for their importation into Microsoft Excel for analysis.

## **4 Results and Discussion**

### **4.1 Ultrasound Imaging of the Phantom Model**

This section details the images obtained from the femur model and the effects of using different ultrasound coupling media.

#### **4.1.1 Ultrasound Gel Coupling**

For practicing techniques, a phantom model of the femur made from rigid polyurethane was used. From the images obtained, Figure 4.1.1, it can be seen that using a free phantom model coupled with ultrasonic gel produced clear images without the effects of ringing artifacts. The bright white semi-circular line followed directly by a shadow can be easily identified as the femoral head. This white line was produced by the reflected ultrasound waves from the underlying surface of the femoral head. The deflected waves then formed a shadow right under its underlying surface. As the waves could not penetrate through the rigid plastic, details of the inner surface were not imaged.

In the case where the tissue mimicking material (wheat-flour adhesive) was used to submerge the plastic femur, both the image resolution and clarity were drastically reduced. In an attempt to obtain better images using the tissue mimicking solution, the gain-compensation of the ultrasound device was further reduced from 40% to 20%, Figure 4.1.1c. This provided better imaging of the femoral head; a bright semi-circle could be easily visualized without the high image ringing artifacts that were present in the images obtained from the 40% gain compensation.



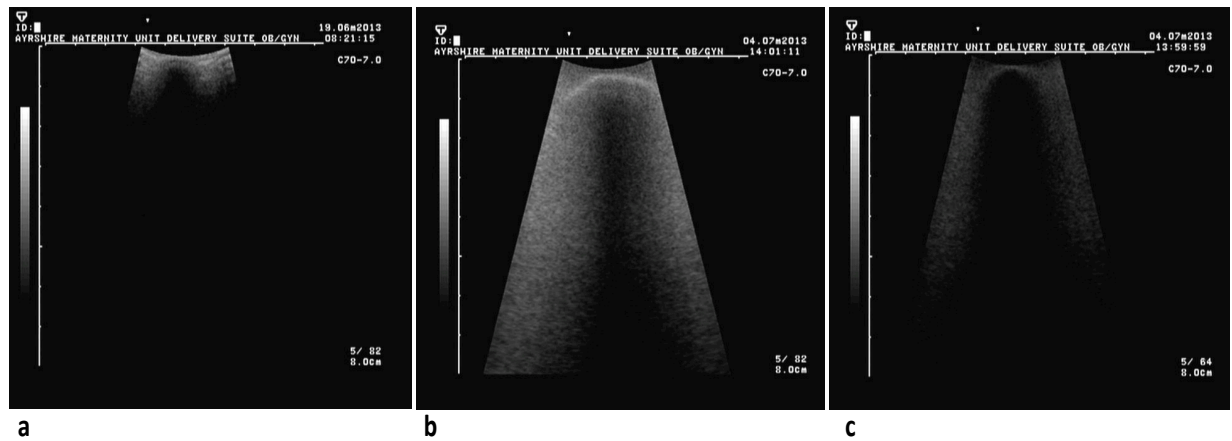


**Figure 4.1.1:** Toshiba SSA-325A images of the Femur Model; (a) without tissue mimicking material; (b) with tissue mimicking material using 40% gain compensation; (c) with tissue mimicking material using 20% gain compensation

#### 4.1.2 Water Bath Submersion

Although the ultrasonic gel provided clear images, it was not that convenient as large quantities of the gel were required to cover the area needed for scanning. Using a water bath eliminated this issue. The images obtained by submerging the femur model into water produced excellent resolution, clarity and contrast, Figure 4.1.2. Using the same gain-compensation of 40%, the images were completely free from ringing artifacts and could be easily used for interpretation and image processing.

To determine whether moving the ultrasound probe around the femur model would be beneficial, i.e. generate better images, two different tests were conducted. From the first series of tests, an unfixed or free model of the femur was used. In this case the ultrasound probe was held in position and the femoral head was manually rotated. The images generated by these trials have a higher resolution in comparison to the images obtained from the femoral model fixed in position with screws, Figure 4.1.2a and 4.1.2b. The images that were obtained from the fixed femur show to have a poorer resolution and were subjected to high ringing artifacts, Figure 4.1.2c and 4.1.2d.

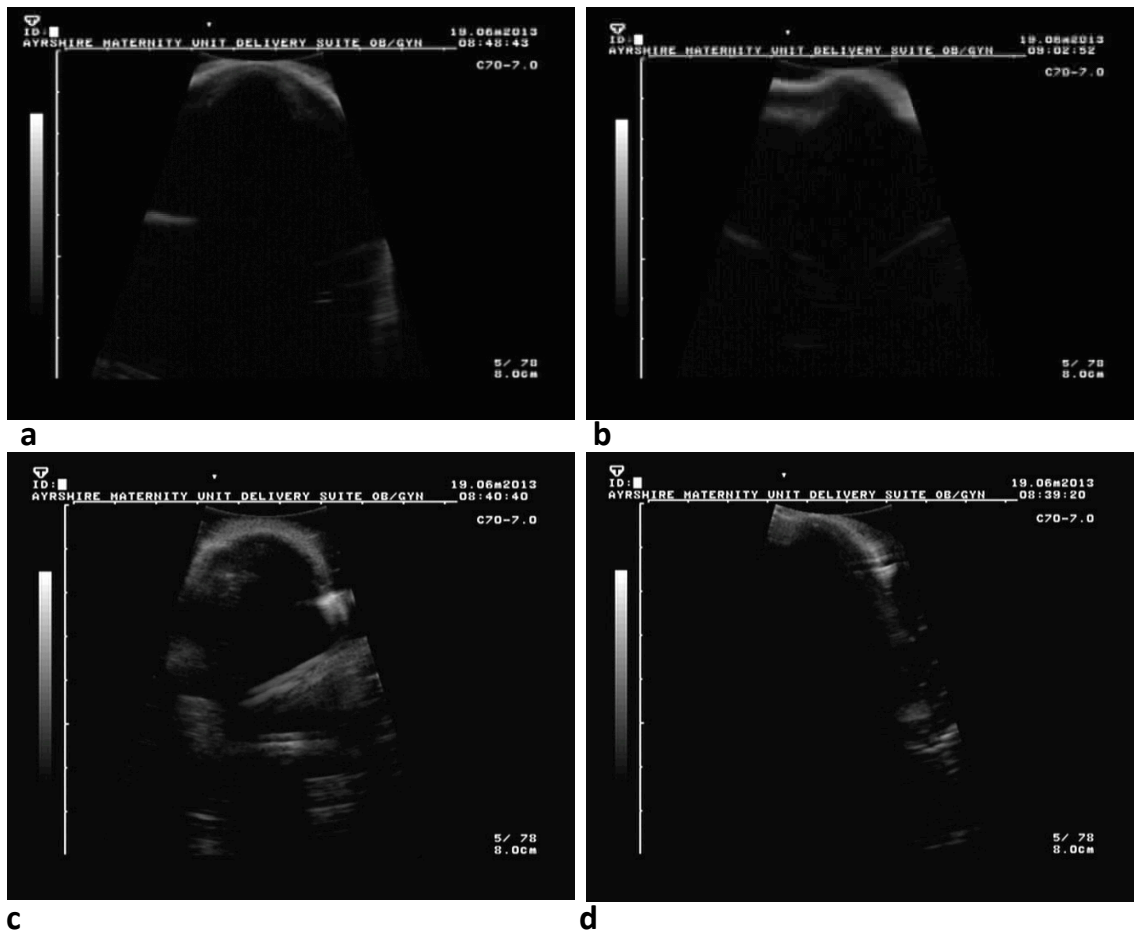


**Figure 4.1.2:** Toshiba SSA-325A images of the Femur Model in a water bath; (a, b) Femoral Head and Shaft in a water bath: unfixed position; (c, d) Femoral Head and Shaft in a water bath: fixed position

It can then be confirmed that by keeping the ultrasound probe in one position limits the degree of image ringing artifacts. This can be mainly associated with the fact that having the probe in a fixed position reduced the error associated with lack or missing interface contact. In other words, in such cases the probe is continuously in full contact with not only the femur model but also with the coupling media. In cases where the ultrasound probe is made to rotate at various angles, the direct interface contact between the femur model and the probe is at times lost partially due to the uneven surface distribution of the model itself, causing decoupling of the matching layer to the target resulting in higher ringing artifacts.

To obtain more realistic images of the femur model, tissue mimicking material made from wheat-flour adhesive was also investigated using a water bath. However, as wheat flour adhesive is water soluble, the experiment was unsuccessful. The tissue mimicking medium surrounding the femur head was simply diluted with its submersion in the water bath, proving to be unreliable.

## **4.2 Ultrasound Imaging of the Subject**

In order to validate the images obtained from the phantom model, a subject's hip area was scanned. Ultrasonic gel coupling was used to produce the images in Figure 4.2. It can be seen that the images obtained using the Toshiba SSA-325A, produced similar results to the phantom model described in Section 4.1.1. The subject's femoral head is slightly visible as a curved white line, followed directly by a shadow. However, the images obtained using the gain-compensation of 40% were not as clear as the ones obtained using the phantom model. This is mainly attributed to the fact that large volumes of tissue such as ligaments, muscles and fat surrounded the subject's hip joint. It is important to note that although the images were not as clear as the ones obtained from the phantom model, they are quite reliable as the head of the femur can be easily identified.

To improve image resolution and to obtain clearer images of the hip joint, two newly manufactured ultrasound machines were tested: Zonare Z.one and Ultrasonix Tablet. Unlike the images obtained from the Toshiba SSA-325A, these images detail more of the underlying tissue surrounding the hip joint; layers of muscles and ligaments can be easily visualized, Figures 4.2c and 4.2d. Although both the Zonare Z.one and Ultrasonix Tablet had great ability to highlight and detail tissue structures, neither were able to clearly underline the head of the femur. The subject's femoral head can be faintly seen at the

bottom of these images with layers of overlying tissue.

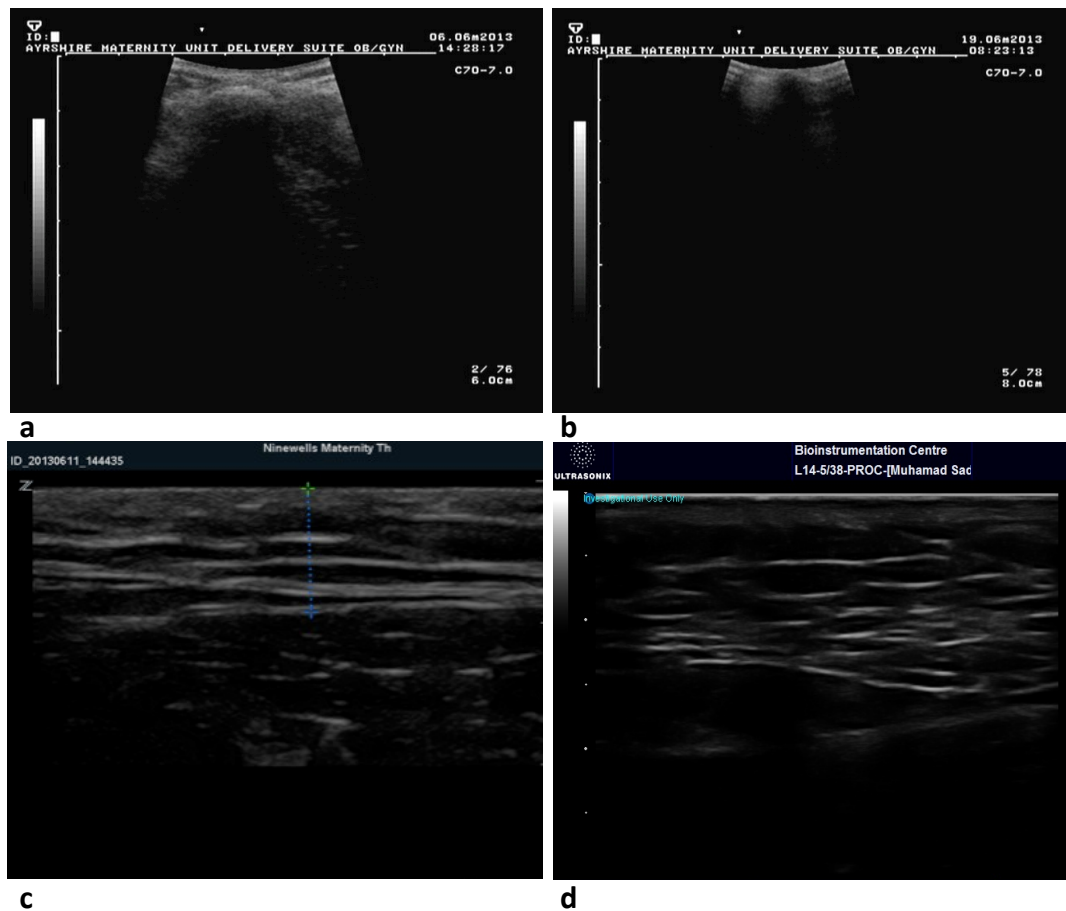


**Figure 4.2:** Ultrasound images of the subject's Hip Joint (a) Toshiba SSA-325A: Femoral Head; (b) Toshiba SSA-325A: Femoral Shaft; (c) Zonare z.one; (d) Ultrasonix Tablet

These images confirm the fact that new ultrasound machines have an increased ability in generating fine details, which can be highly beneficial for blood vessel and organ tracking; however, they do not have a great advantage for imaging bone. The main benefit of using such newly developed ultrasound devices for imaging bone are their ability to reduce scanning times and their ability to store different digitalized data formats without the need of using external data processors.

### 4.3 Location of the HJC using Ultrasound Imaging

The Mimics 12.01 Software described in Section 3.5, was incompatible with the images obtained from the Toshiba SSA-325A Ultrasound. Although the videos and images

obtained were converted into JPEG format, the 12.01 version was not robust enough to import the images saved. Various image modifications were carried out in an attempt to make the software read the imported data.

The images were first cropped to display only the targeted region of the femoral head. They were then compressed from 850KB to 450KB and saved as BMP, refer to Appendix C for the image modifications. However, this compression in file size did not have much benefit. Converting the images to BMP caused the files to be saved with different sizes, adding another complication for the Mimics software as it could only download and import data of equal file size. Therefore, MATLAB was used to re-save the BMP images all to an equal size, refer to Appendix D for the re-sizing image code. Re-saving the images with identical dimensions of 380 x 345mm allowed their importation into the Mimics software.

The ultrasound scans obtained from the subject were segmented to create a 3D model, Figure 4.3A. However, from the model generated only a partial structure of the femoral head was visible and the subject HJC could not be identified. This can be mainly associated with the fact that ultrasound imaging does not involve slice reconstruction; it simply provides real-time view of the underlying structure. In addition, as the transducer itself could not be made to physically rotate around the subject's HJC, a complete 3D model of the hip joint could not be generated; therefore, only generalized view of the femur head was obtained.

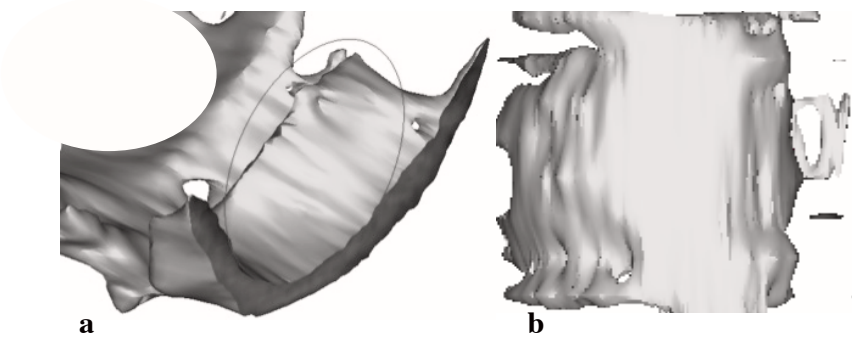


**Figure 4.3A:** 3D model of Femoral Head (a) Frontal View; (b) Rear View

To externally locate the HJC, the diameter of the head of the femur was first calculated and the distance of the two ends of the probe in relation to the RPSIS and RASIS were then obtained from the reflective markers placed on the probe using the Vicon motion capture system.

To determine the diameter of the femoral head, the distance/density tool command in the Mimics software was used. This allowed for the calculation of two identified points, Figure 4.3B(a). To determine the accuracy of the 69.38mm diameter obtained from the two identified points, based on the assumption that the hip joint resembles a ball and socket joint, a circle was then drawn around the femoral head and a diameter of 69.86mm was obtained, Figure 4.3B(b). As both methods gave a similar result with a mean difference of  $0.48 \pm \text{mm}$ , 69mm was taken as the diameter of the femoral head, despite its slight oversize.

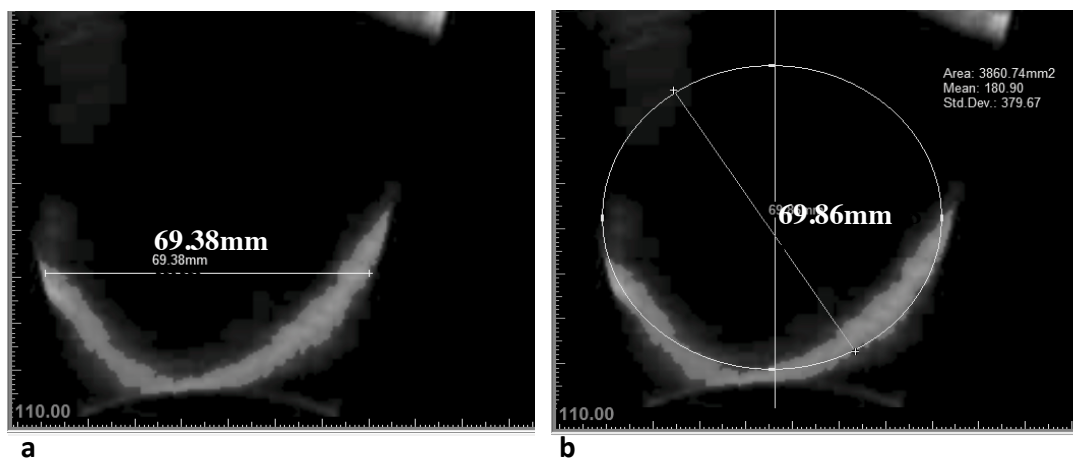


**Figure 4.3B:** Diameter of the Femoral head (a) Constructed line; (b) Constructed Circle

The static data obtained from the Vicon system was then used to calculate the distance from the ends of the probe to both the RPSIS and RASIS. Knowing both the radius of the femoral head and the distance of the probe from the pelvis's bony landmarks, the HJC could be identified externally on the body. Table 4.3 summarizes the results obtained.

**Table 4.3: HJC Distance from ASIS and PSIS**

	Distance to RASIS (mm)			Distance to RPSIS (mm)		
	x	y	z	x	y	z
<b>Transducer (Probe) End 1</b>	35.009	25.663	27.8	144.527	66.303	81.514
<b>Transducer (Probe) End 2</b>	24.180	27.174	26.684	155.354	67.815	27.029
<b>HJC</b>	64.095	60.919	61.742	184.442	101.559	61.528

### **Sample Calculation**

(1) Distance from Transducer End 1 to RASIS:

$$\text{Distance } (x,y,z) = \frac{\sum_{n=1}^n [\text{Position } (x,y,z) \text{ Transducer End 1} - \text{Position } (x,y,z) \text{ RASIS marker}]}{n} \quad (4.3a)$$

where n = number of trails

(2) Distance from the HJC to RASIS:

$$\text{HJC Location} = \sum \frac{(\text{Radius of Femoral head} + \text{Position of Trasducer Ends})}{2} \quad (4.3b)$$

## **4.4 Functional Method Validation**

In order to determine the accuracy of using an ultrasound device for locating the HJC, the functional method proposed by Gamage and Lasenby was used. The MATLAB code described in Section 3.9 was applied to the data obtained from the circumduction of the subject's right leg. As the local coordinate system proposed by Wu *et al* [16] assumes orthogonal axis, the code was modified to produce orthogonal results. The origin of the

local coordinate system was located at the right ASIS instead of the pelvis centre so that it could be validated using ultrasound testing on the subject’s right leg.

The centre of rotation of the subject’s hip joint was obtained by averaging the trajectories common to all the thigh makers and the spherical radii of each marker produced by the trajectories were computed.

#### 4.4.1 Placement of Markers on the Subject’s Skin

As with last years project, the retro-reflective markers were first placed directly on the subject’s skin, Table 4.4.1 summarizes the results obtained. These results are comparable to ones obtained last years. It can be noted the individual markers had a bias in the order of  $10^{-2}$ , from this it was confirmed that the results, although not exact, were accurate enough to be analyzed.

**Table 4.4.1:** HJC location using Gamage and Lasenby’s Functional Method

	Thigh Lateral Marker 1	Thigh Anterior Marker 1	Thigh Lateral Marker 2	Thigh Anterior Marker 2
<b>Radii of thigh markers (mm)</b>	199.42	270.02	167.95	242.79
<b>Minimum Radii (mm)</b>	191.28	263.35	159.02	236.00
<b>Maximum Radii (mm)</b>	209.70	280.20	178.16	251.93
<b>Bias</b>	$-3.34 \times 10^{-2}$	$-2.53 \times 10^{-2}$	$-3.22 \times 10^{-2}$	$-1.67 \times 10^{-2}$
<b>Centre of Rotation (HJC) (mm)</b>	$\begin{bmatrix} -24.26 \\ 121.16 \\ -223.84 \end{bmatrix}$			

It can also be noted that the “Thigh Anterior Marker” produced the largest difference between the maximum and minimum radii of the thigh markers, which is in accordance with Comomilla *et al* findings. This 19.14mm difference can be related to the higher



presence of STAs in the anterior area compared to the lateral area of the thigh.

The marker trajectories in the Global and Local Coordinate System can be seen in Figures 4.4.1A and 4.4.1B respectively. Figure 4.4.1A, only plots two of the four thigh markers for clarity. From the Local Coordinate System, Figure 4.4.1B, the trajectories of the individual thigh markers can be visualized on their relative spheres.

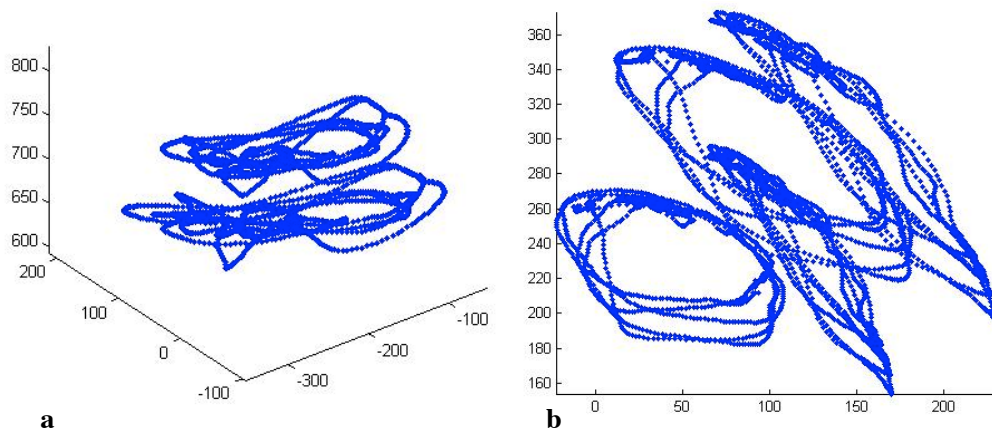


**Figure 4.4.1A:** Reflective marker trajectories of the thigh in Global Coordinate System

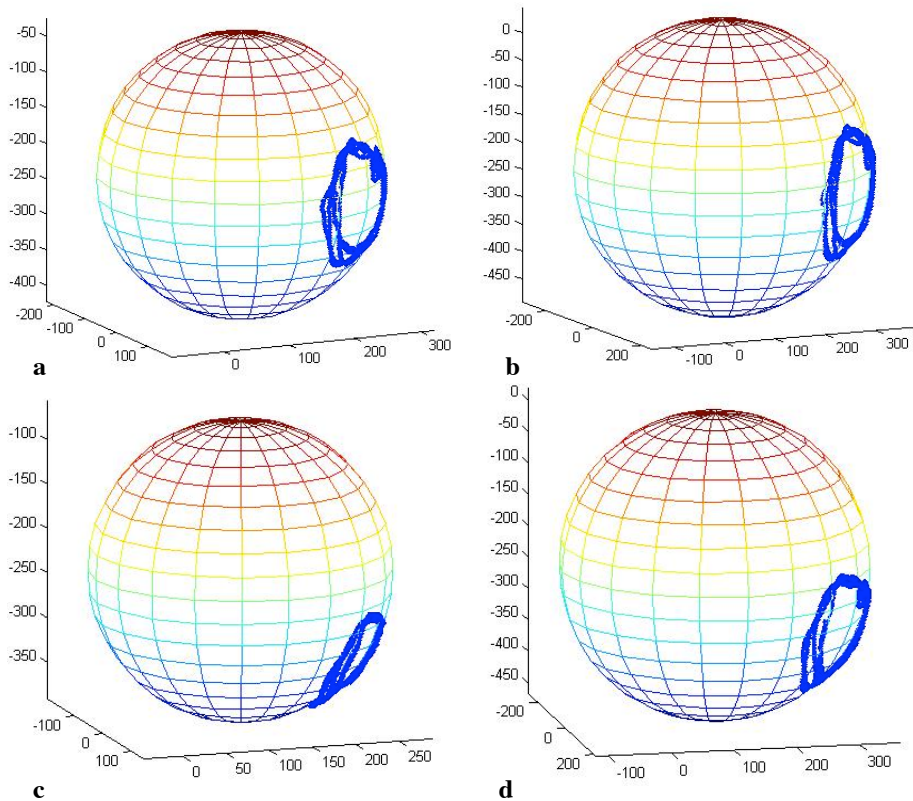


**Figure 4.4.1B:** Reflective marker trajectories of the thigh in Local Coordinate System

#### 4.4.2 Placement of Markers on a Cotton Strap

In an attempt to reduce the effects of STA, the experiment was re-conducted by positioning the reflective markers on a cotton strap placed around the subject's waist and thigh, Table 4.4.2 summarizes the results obtained. From the results, it can be noted the individual markers had a bias in the order of  $10^{-3}$ ; this is a hundred fold reduction in comparison to the placement of the markers directly on the skin.

*Table 4.4.2: HJC location using Gamage and Lasenby's Functional Methods*

	<b>Thigh Lateral Marker 1</b>	<b>Thigh Anterior Marker 1</b>	<b>Thigh Lateral Marker 2</b>	<b>Thigh Anterior Marker 2</b>
<b>Radii of thigh markers (mm)</b>	218.89	288.25	186.40	261.4455
<b>Minimum Radii (mm)</b>	212.95	281.86	181.97	257.05
<b>Maximum Radii (mm)</b>	226.07	295.03	190.36	266.11
<b>Bias</b>	$7.11 \times 10^{-3}$	$6.28 \times 10^{-3}$	$9.71 \times 10^{-3}$	$4.38 \times 10^{-3}$
<b>Centre of Rotation (HJC) (mm)</b>	$\begin{bmatrix} -42.64 \\ 117.79 \\ -227.29 \end{bmatrix}$			

It can also be noted that the "Thigh Anterior Marker", like the case where the markers were placed directly on the skin, produced the largest difference between the maximum and minimum radii of the thigh markers. However, this difference was reduced from 19.4mm to 13.12mm. This decrease in 6.02mm proves that by placing the markers on a strap, rather than the skin directly, reduces the effects of STA producing more accurate results.

It should be noted that the y and z coordinates of the centre of the hip joint was comparable to the y and z coordinated obtained in Section 4.4.1. However, the x coordinate was slightly shifted. This shift can be directly linked to the degree of movement of the retro-reflective markers. The positioning of the markers on the skin caused more movement as the double-sided tape was not able to firmly stick to the subject's leg, causing the markers to slightly

shift from their original position. However, using the cotton strap eliminated this problem as the markers were held firmly in position, preventing their movement.

The marker trajectories in the Global and Local Coordinate System can be seen in Figures 4.4.2A and 4.4.2B respectively. Figure 4.4.2A, as in Section 4.4.1, only plots two of the four thigh markers for clarity purposes. From the Local Coordinate System, Figure 4.4.2B, the trajectories of the individual thigh markers can be visualized on their relative spheres.

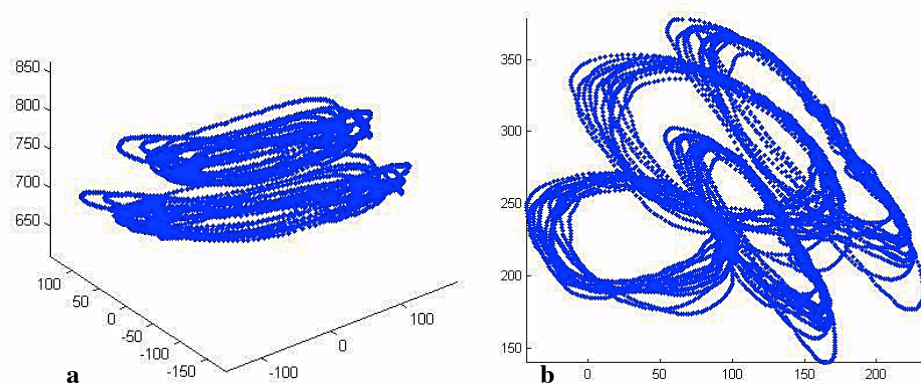


**Figure 4.4.2A:** Reflective marker trajectories of the thigh in the Global Coordinate System

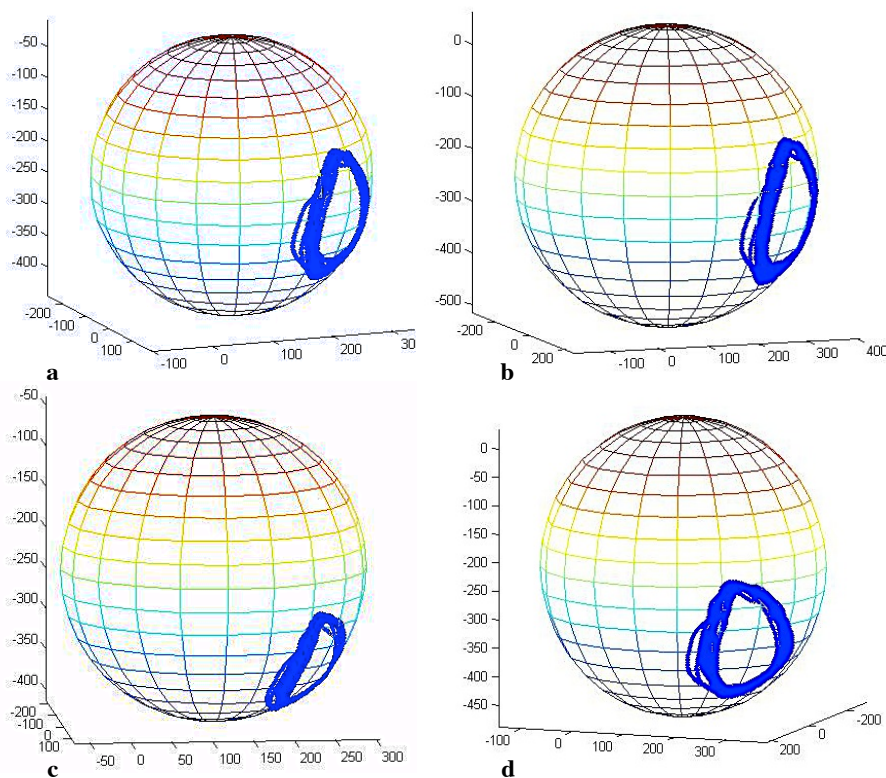


**Figure 4.4.2B:** Reflective marker trajectories of the thigh in the Local Coordinate System

#### 4.5 Ultrasound and Functional Method Comparison

Although the Mimics 12.01 software was unable to fully reconstruct the ultrasound images to obtain a full 3D model, the diameter of the femoral head and subsequently the distance of the HJC from the PASIS and RASIS were roughly estimated. A summary of the results obtained from both the ultrasound and functional methods are presented in Table 4.5.

*Table 4.5: Summary of the results obtained for the location of the HJC*

	HJC (mm)		
	x	y	z
<b>Mimics 12.01 (Distance to RASIS)</b>	64.095	60.919	61.742
<b>Mimics 12.01 (Distance to PSIS)</b>	184.442	101.559	61.528
<b>Gamage and Lasenby (without strap)</b>	-24.26	121.16	-223.84
<b>Gamage and Lasenby (with strap)</b>	-42.64	117.79	-227.29

From the results obtained it can be noted that apart from the variations obtained from the two trials using Gamage and Lasenby's regression equations, as described in Section 4.4, these results are highly different from the ones calculated from the ultrasound images obtained from the Mimics 12.01 software.

This large discrepancy between the data obtained from the ultrasound scans and the functional method lies in the fact that the functional method used located the HJC was in relation to the centre of rotation of the hip, in other words, it calculated the rotation of the hip and identified its centre based on the leg's trajectories, building a local coordinate system. Whereas, the ultrasound scans that were imported into the Mimics 12.01 software, could only be used to calculate a rough estimate between the distance of the hip joint and the bony landmark of the pelvis. Therefore, a direct comparison could not be made between the two methods obtained.

The inability of the Mimics 12.01 software to generate a complete 3D model of the hip joint to calculate and establish a coordinate system was the main reason for this lack of comparison.

## **5 Conclusion**

This study shows that the use of ultrasounds to determine a local coordinate system that can locate the HJC is relatively straightforward. However, proper image processing techniques are required to obtain reliable results. Creating 3D images that can be used to establish a local coordinate system will alleviate the issue of subjective ultrasound image analyses.

Although a direct comparison could not be made between the ultrasound and the functional verification method, this study shows the discrepancies that exist in locating the HJC. These discrepancies are mainly associated with the presence of STA. The fact that functional methods are still widely used and accepted in clinical settings despite their accuracy is highly alarming.

The conclusions from this study confirm the lack of proper techniques that are currently available to create a local coordinate system to locate the HJC due to the presence of STAs and detail the advantages of replacing these methods with medical equipment, in particular ultrasounds, as they can elevate the errors related to STAs producing more accurate results.

## **6 Future Work**

This research shows that the issue of locating the HJC is still quite prominent mainly due to the fact the hip joint itself is situated deeply in pelvis surrounded by large volumes of soft tissue. Although the use of ultrasonic devices for locating the HJC is promising as it reduces the errors associated with STAs, a lot more research has to be carried out before they can be used in clinical settings as the gold standard for locating the HJC.

### **6.1 Improvements in Ultrasonic Techniques**

To improve the accuracy of ultrasonic devices, further investigations should be carried out using image processing techniques to attempt to create 3D ultrasound imaging in real time; eliminating the issue of subjective image interpretations. For better image quality and resolution, the use of a water bath as a substitute for the standard ultrasonic gel media can further be studied to improve the contact interface between the ultrasound probe and skin.

In addition, various tissue mimicking materials can be further looked into. This will allow the creation of phantom models that precisely replicate the tendons, muscles and ligaments that are present around the femoral head under the skin. Such materials would have to undergo changes in their physical properties once positioned around the phantom model. Ideally the media should not be water-soluble after it settles, eliminating the issue of solubility. This will allow ultrasound imaging using water baths.

Tissue mimicking materials that are currently being used by other research groups such as vessel modeling can be further investigated. In particular the use of PolyVinyl Alcohol (PVA) and hydrogels made from agar look highly promising. Although PVA is quite expensive, it has the ability to undergo changes in its physical property behaving like a gel

once it dissolves in water and settles at -20°C. Hydrogels made from agar, although quite fragile, have excellent tissue mimicking property making them a good substitute from the wheat flour adhesive used in this study.

## **6.2 Improvements for Ultrasonic Image Processing**

Although the Mimics 12.01 software used provided a general idea of the location of the HJC centre, a lot more testing must be carried out to determine whether using such a system is feasible. Looking into ways of constructing 3D imaging in real time will provide a solid step for determining the HJC that would eliminate the problems of subjective image interpretation.

In order to be able to reconstruct 3D models of the ultrasound images obtained, the newer Mimics<sup>16</sup> software can be used and tested for ultrasound image processing. Nevertheless, no guarantee can be made whether this version would be able to import the ultrasound images without the need for image modification. The main challenge is that the images obtained from ultrasounds are different in nature to the ones obtained from MRI and CT scans; they do not involve slice image reconstruction of the underlying structure. It is therefore unclear whether these software can construct complete 3D models from continuous imaging obtained from ultrasounds. It would however provide an indication of whether such software that are currently being used in medical settings for MRI and CT scans could also be used for ultrasound imaging.

## **6.3 Improvements for Data Acquisition using Functional Methods**

Although functional methods based on Gamage and Lasenby provide a good estimation of the location of the HJC as a validation technique, further investigation should be made to



reduce the effects of STA mainly caused by the movements of the retro-reflective markers positioned on the skin.

The use of a band or strap made from a material that is both water and oil resistant can be further investigated. In theory such materials, such as Neoprene, would not only have the ability to stay in place, without worrying about the effects of skin sweating, but the reflective markers will also be held firmly in position with minimal movement due to vibration. The main issue with directly positioning the markers on the skin is that they are constantly subjected to movement, which is caused by skin stretching and muscle contraction along the hip and thigh region. Although the use of a cotton strap in this study showed to be beneficial reducing bias down to  $10^{-3}$ , it is still far from accurate.

## References

- [1] Szabo T.L. “*Diagnostic Ultrasound Imaging: Inside out*”. Elsevier Academic Press: Burlington 2004, pp. 5-27
- [2] Baxter G.M. “*Clinical Diagnostic Ultrasound*” Wiley: Boston 1999 pp. 34-60
- [3] Bhargava S.K. “*Principles and Practices of Ultrasonography*”. Alpha Science International: New York 2003 pp. 50-78
- [4] Overhoffa H.M, Lazovicb D, Jan U. “*Visualization of the newborn’s hip joint using 3-D ultrasound and automatic image processing*”. Hildesheim: Medical School of Hannover
- [5] Gill R. “*The Physics and Technology of Diagnostic Ultrasound: A Practitioner's Guide*”. High Frequency Publishing: Sydney 2012, pp. 67-100
- [6] Kremkau F.W “*Diagnostic Ultrasound: Principles And Instruments*”. Elsevier: San Francisco 2006 pp.20-32
- [7] Bluth E.I , Arger P.H, Benson C.B, Ralls P.W, Siegel M.J “*Ultrasound: A Practical Approach to clinical problems.*” Thieme: New York 2000, pp. 135-153
- [8] Ultran Laboratories, Inc. High transduction Piezoelectric transducers and introduction of Non-Contact analysis. Available at: <http://www.ndt.net/article/v05n01/bhardwaj/bhardwaj.htm>. Accessed June1st 2013
- [9] Williams L. “The Ultrasound”. Available at: <http://www.msdlatinamerica.com/ebooks/CoreCurriculumTheUltrasound/sid102252.html>. Accessed June1st 2013
- [10] Luís del Cura J, Segui P, Nicolau C. “*Learning Ultrasound Imaging*”. Springer-Verlag: Berlin Heidleberg 2012, pp. 52-60
- [11] Piazza S.J, Erdemir A, Okita N, Cavanagh P.R. “*Assessment of the functional method of hip joint centre location subject to reduced range of hip motion*”. Journal of Biomechanics 2004, Vol.34 pp. 349-356
- [12] Martini F, Nath J. “*Fundamentals of Anatomy & Physiology: Ninth Edition*”. Pearson Education: San Francisco 2012 pp. 262-263.
- [13] Medical Dictionary. “Anatomy of the Hip Joint”. [http://medical-dictionary.thefreedictionary.com/Hip+\(anatomy\)](http://medical-dictionary.thefreedictionary.com/Hip+(anatomy)) Accessed June10th 2013
- [14] Grood E.S, Suntay W.J. “*A joint coordinate system for the clinical description of three-dimensional motions: application to the knee*”. Journal of Biomechanical Engineering 1983: Vol105 pp.136-144
- [15] Seidel G. K, Marchinda D. M, Dijkers M, Soutas-Little R. W. “*Hip Joint Centre Location From Palpable Bony Landmarks-A Cadaver Study*”. Journal of

Biomechanics 1995: Vol28 pp. 995-998

- [16] WU G.E. *ISB Recommendation on Definition of Joint Coordinate System of Various Joints for the reporting of Human Joint Motion-Part I: ankle, hip and spine*. Journal of Biomechanics 2002, Vol.35, pp. 543-548
- [17] Stagni R, Fantozzi S, Cappello A, Leardini A. “*Quantification of soft tissue artefact in motion analysis by combining 3D fluoroscopy and stereophotogrammetry: a study on two subjects*”. Clinical Biomechanics 2005: Vol20 pp. 320-329
- [18] Kratzstein S, Kornaropoulos E.I, Ehrig R.M, Heller M.O, Pöppelau B.M, Taylor W.R. “*Effective marker placement for functional identification of the centre of rotation at the hip*”. Gait and Posture 2012: Vol36 pp. 482-486
- [19] Camomilla V, Cereatti A, Cheze L, Cappozzo A. “*A hip joint kinematics driven model for the generation of realistic thigh soft tissue artefacts*”. Journal of Biomechanics 2012 Vol46 pp. 625-630
- [20] Bell A, Brand R, Pedersen D. “*Prediction of hip joint centre location from external landmarks*”. Human Movement science 1989: Vol.8, pp. 3-16.
- [21] Bell A, Pedersen D, Brand R. “*A comparison of the accuracy of several hip centre location prediction methods*”. Journal of Biomechanics 1990: Vol.23, pp. 617-621
- [22] Davis R, Öunpuu S, Tyburski D, Gage J. “*A gait analysis data collection and reduction technique*”. Human Movement Science 1991: Vol.10 pp. 171-178
- [23] Leardini A, Cappozzo A, Catani F, Toksvig-larsen S, Petitto A, Sforza V, Cassanelli G, Giannini S. “*Validation of a functional method for estimation of hip joint centre location*”. Journal of Biomechanics 1999: Vol32, pp. 99-103
- [24] Harrington M, Zavatsky A.B, Lawson S.E, Yuan Z, Theologis T.N. “*Prediction of the hip joint centre in adults, children and patients with cerebral palsy based on magnetic resonance imaging*”. Journal of Biomechanics 2007: Vol.40, pp. 595-602
- [25] Lucchetti L, Cappozzo A, Cappello A, Croce U. “*Skin movement artefact assessment and compensation in the estimation of knee-joint kinematics*”. Journal of Biomechanics 1998: Vol.31, pp. 977-984
- [26] Gamage S, Lasenby J. “*New least squares solutions for estimating the average centre of rotation and axis of rotation*”. Journal of Biomechanics 2002: Vol.35, pp. 87-93.
- [27] Ehrig R.M, Heller M.O, Kratzstein S, Duda G.N, Trepczynski A, Taylor W.R: “*The SCoRE residual: A quality index to assess the accuracy of joint estimations*”. Journal of Biomechanics 2011: Vol44, pp. 1400-1404
- [28] Suryanarayana C, Grant Norton M. “*X-Ray Diffraction: A Practical Approach*”.

Plenum Press: New York 1998 pp. 5-18

- [29] Mark A. Brown M.A , Semelka R.C. “*MRI: Basic Principles and Applications*”. Wiley-Blackwell: New jersey 2010 pp.49-69
- [30] Vivian Gibbs V, Cole D, Sassano A. “*Ultrasound Physics and Technology: How, Why, and when*”. Elsevier: New York 2009 pp. 7-39
- [31] Rowbotham E.L, Grainger A. “*Ultrasound-Guided Intervention Around the Hip Joint*”. American Roentgen Ray Society 2010: Vol.10 pp. 122-128
- [32] Blaivas, M. et al., 2004. Water bath evaluation technique for emergency ultrasound of painful superficial structures. *The American Journal of Emergency Medicine*, 22(7), p. 589–593.
- [33] Hicks, J. and J. Richards, "Clinical applicability of using spherical fitting to find hip joint centres". *Gait and Posture* 2005: Vol.22, pp. 138-145
- [34] Peters A, Baker R, Sangeux M. “*Validation of 3-D freehand ultrasound for the determination of the hip joint centre*”. *Gait and Posture* 2010: Vol.31 pp. 530–532
- [35] Hsu P.W, Treece G.M, Prager RW, Houghton N.E, Gee A.H. “*Comparison of Freehand 3D Ultrasound Calibration Techniques Using a Stylus*”. Cambridge: University of Cambridge 2007
- [36] Peters A, Baker R, Morris M.E, Sangeux M. “A comparison of hip joint centre localization techniques with 3-DUS for clinical gait analysis in children with cerebral palsy”. *Gait and Posture* 2012: Vol.36, pp. 282-286
- [37] Lasaygues P, Lefebvre J. “*New Deal and Prospects in Long-Bone Ultrasonic Imaging*”. IEEE Ultrasonic Symposium 2001 Vol.2, pp. 1209-1212
- [38] The Hong Kong Polytechnic University. *3D Ultrasound Imaging*. Available at: [www.acad.polyu.edu.hk/~rcbus/3DUltrasoundImaging/Introduction.htm](http://www.acad.polyu.edu.hk/~rcbus/3DUltrasoundImaging/Introduction.htm). Accessed 27 June 2013
- [39] Heller M.O, Matziolis G, König C, Taylor W.R, Hinterwimmer S, Graichen H, Hege H.C, Bergmann G, Perka C, Duda G.N. “*Musculoskeletal Biomechanics of the Knee Joint*”. *Journal of Orthopedics* 2007 Vol36, pp.628-623
- [40] Romana T. “*Prediction of the Hip Joint Centre by predictive methods, Functional methods and Ultrasound imaging technique*”. Glasgow: University of Strathclyde 2012
- [41] Simpson C. “*Prediction of the Hip Joint Centre from Externally Placed Markers in Gait Analysis Studies*”. Glasgow: University of Strathclyde 2011

## Appendices

### Appendix A: University of Strathclyde's Codes and Guidelines

The following section provides the Ethics Form, Consent Information and E-mail that was prepared and sent to recruit a subject for this experiment.

#### Ethics Form

1. Title of the investigation Locating the Hip Joint using Ultrasonic Techniques
2. Chief Investigator (Ordinance 16 member of staff only) Name: Stephanos Solomonidis Status: <input type="checkbox"/> Professor <input type="checkbox"/> Reader <input checked="" type="checkbox"/> Senior Lecturer <input type="checkbox"/> Lecturer Department: Biomedical Engineering Telephone: [REDACTED] E-mail: [REDACTED]
3. Other Strathclyde investigator(s) Name: Mona Tahvildar-Khazaneh Status (e.g. lecturer, post-/undergraduate): Postgraduate Department: Biomedical Engineering Telephone: [REDACTED] E-mail: [REDACTED]
4. Non-Strathclyde collaborating investigator(s) Name: George Corner Status (e.g. lecturer, post-/undergraduate): Lecturer Department/Institution: University of Dundee If student(s), name of supervisor: Telephone: [REDACTED] E-mail: [REDACTED] Please provide details for all investigators involved in the study: Head of Instrumentation: Medical Physics Department Ninewells Hospital and Medical School Dundee
5. Overseas Supervisor(s) <b>N/A</b> Name(s): Status: Department/Institution: Telephone: Email: I can confirm that the local supervisor has obtained a copy of the Code of Practice: Yes <input type="checkbox"/> No <input type="checkbox"/> Please provide details for all supervisors involved in the study:
6. Where will the investigation be conducted Bioengineering unit: Gait Laboratory

7. Duration of the investigation

Duration(years/months) : 1 month

Start date (expected): Subject testing 10/07/2013  
08 / 2013

Completion date (expected): 01 /

8. Sponsor (please refer to Section C and Annex 3 of the Code of Practice):

University of Strathclyde

9. Funding body (if applicable) **N/A**

Name of funding body:

Status of proposal – if seeking funding (please click appropriate box):

In preparation

Submitted

Accepted

Date of Submission of proposal: / /

Date of start of funding: / /

10. Objectives of investigation (including the academic rationale and justification for the investigation)

In order to determine sufficiently and accurately kinematic and kinetic data during studies of human motion, the location of the centre of rotation of various joints of the lower limb should be located as accurately as possible. Although the knee and ankle joints can be determined reasonably well by palpation, the hip joint centre is difficult to locate being situated deeply in the pelvis.

The HJC (Hip Joint Centre) is normally assessed using predictive and functional methods. However, recent studies have indicated that these test methods are highly inaccurate and unreliable. Predictive methods, which are based on regression models, do not allow for patient customization causing high variations. Functional methods, on the other hand, are based on data obtained from skin markers; however they cannot differentiate between physiological movements of the skin markers over the underlying bone due to muscle contraction and synchronous shifting from soft tissue artefacts.

The use of non-invasive devices such as MRI and ultrasound are promising techniques that can be used for verification of the HJC. However, due to the cost associated with MRI, ultrasound verification will be investigated. The underlying issue with ultrasound is its highly subjective analysis. Therefore, the aim of this project will be to develop a new technique that can be used to assess images that are obtained from an ultrasound. The technique that would be used would involve image processing to try to convert the 2D ultrasound images into 3D images using Mimics Software.

### 11. Nature of the participants

Please note that investigations governed by the Code of Practice that involve any of the types of projects listed in B1(b) must be submitted to the University Ethics Committee for prior approval

Are any of the categories mentioned in Section B1(b) (participant considerations) applicable in this investigation?

Yes

No

Please detail nature of participants:

Number: 1      Age (range): 20+

Please also include information on: recruitment methods (see section B4 of the Code of Practice); inclusion/exclusion criteria; and any further screening procedure to be used

For the recruitment stage, an email (provided as attachment) will be sent out to the student list of the biomedical engineering department, detailing the title of the project and what is required of the participant. Specifically the times that they need to be available and the procedure that will be carried out on them using an ultrasound device will be explained. The email will have the participant information sheet and consent form attached. If the participant wishes to be considered for inclusion in the study the consent form will be returned to the researcher along with contact details, age, height and weight. However the potential participant may also contact the researcher for additional information prior to making the decision to volunteer. This email will allow interested candidates to read the information on their own time, giving them complete control on whether they want to part take in the experiment.

Individuals who are classified as obese cannot part take in this experiment due to a higher incorporation of soft tissue artefact. In order to determine whether the volunteer can be included, their height in meters and mass in kilograms will be taken. Their mass to height ratio will be calculated to determine their Body Mass Index (BMI). If their BMI falls between 18.2-25 then they will be able to participate in the experiment.

As the experiment only involves scanning the hip area and not the pelvis region, the potential of identifying an unknown pregnancy will be zero for a female candidate. Therefore, no preference will be made on the gender of the participant.

### 12. What consents will be sought and how?

Please note that the information sheets and consent forms to be used should be attached to this form

As described in Section 11, an email will be first sent out to the student list of the biomedical engineering department, detailing the project. The required availability of the volunteer and details of what the volunteer is required to do will be specified.

The email will then contain an attachment of a participant information sheet and consent form. Interested participants will then be required to read and sign the form. The participant will have time to consider whether they would like to volunteer in the experiment without feeling obliged or forced.

### 13. Methodology

Investigations governed by the Code of Practice that involve any of the types of projects listed in B1(a) must be submitted to the University Ethics Committee for prior approval. Where an independent reviewer is not used, then the UEC/ DEC reserves the right to scrutinise the methodology.

Are any of the categories mentioned in the Code of Practice Section B1(a) (project considerations) applicable in this investigation?

Yes

No

If 'yes' please detail:

Design: what kind of design/research method(s) is/are to be used in the investigation?

Ultrasound Imaging

Techniques: what specific techniques will be employed and what exactly is required of participants?

The experiments will be similar in nature to the one held last year at the biomedical engineering department at the University of Strathclyde. This experiment involved using an ultrasound probe on a subject's hip region to obtain ultrasonic images for comparison between MRI images obtained from the same area i.e. hip joint.

In this study, the participant will be required to lie still on a bed. Ultrasonic gel will then be placed and spread across the patient's hip area. An ultrasound probe will then be externally positioned around their hip area. The probe will be used to go around the hip area of the subject's leg only; no other area of the subject will be scanned. As the probe will be moved across their hip region, ultrasound images can be simultaneous viewed by both the researcher and the volunteer in real time on the ultrasound monitor screen.

The experiments will be held in the biomedical engineering gait laboratory in the month of July. None of the trials conducted should last longer than 5 minutes, allowing the participant to take breaks in-between the trials as they require. You need to include that there appears to be 5 scans taken on separate days?

Has this methodology been subject to independent scrutiny?

Yes

No

Please provide the name and contact details of the independent reviewer:

#### 14. Data collection, storage and security

Explain how data are handled, specifying whether it will be fully anonymised, pseudo-anonymised, or just confidential, and whether it will be securely destroyed after use:

No names will be taken. An alphabetical letter will be assigned to the volunteer.

Explain how and where it will be stored, who has access to it, and how long it will be stored:

The images obtained from the ultrasound device will be stored on an encrypted flash drive, accessed only by a password. The chief investigator and researcher will only have access to this flash. Once the project is complete the images will be stored on an encrypted disc.

Will anyone other than the named investigators have access to the data? Yes  No

If 'yes' please explain:

#### 15. Potential risks or hazards

No risks are known to be associated with the use of an ultrasound. No diet or exercise is required for preparation.

However, in the case of identifying anything abnormal in the ultrasound images, the participant will be referred to their General Practitioner (GP).

#### 16. Ethical issues

A burden the volunteer may face is changing into shorts before the experiments.

#### 17. Any payment to be made

No

#### 18. What debriefing, if any, will be given to participants

No feedback will be provided to the participant on the images obtained; however, if anything unusual is found on their ultrasound images, they will be referred to their GP. A summary of how the images have helped in locating the hip joint will be provided on request.

#### 19. How will the outcomes of the study be disseminated (will you seek to publish the results)

The images obtained from the volunteer's hip joint will be published in a MSc thesis project. The images obtained will be compared with other techniques used in clinical settings to assess the accuracy when using ultrasound devices.



20. Nominated person to whom participants' concerns/ questions should be directed before, during or after the investigation (please also provide contact details)

Mr. Stephan Solomonidis  
Biomedical Engineering Unit  
University of Strathclyde  
106 Rottenrow,  
Glasgow G4 0NW  
Telephone: 0141 548 3778  
Fax: [REDACTED]  
Email: [REDACTED]

21. Previous experience of the investigator(s) with the procedures involved

Stephan Solomonidis: Has studied and has experimented alternative ways of locating the hip joint centre using both clinical devices and established algorithms for many years. He will be providing direct feedback on the outline and procedure of this project.

George Corner: Has collaborated with some preliminary tests carried out last year at Ninewells Hospital. He has extensive experience on clinical ultrasonics. He will be providing advice on the procedures of this project.

Mona Tahvildar-Khazaneh: Has recently gained experience using Ultrasound machines from carrying out trials on a plastic hip model. She will be in charge of obtaining images from the participant's hip area, and comparing the results with current methods used in clinical settings.

Checklist	Enclosed	N/A
Participant Information Sheet(s)	<input checked="" type="checkbox"/>	<input type="checkbox"/>
Consent Form(s)	<input checked="" type="checkbox"/>	<input type="checkbox"/>
Sample questionnaire(s)	<input type="checkbox"/>	<input checked="" type="checkbox"/>
Sample interview format(s)	<input type="checkbox"/>	<input checked="" type="checkbox"/>
Sample advertisement(s)	<input type="checkbox"/>	<input checked="" type="checkbox"/>
Any other documents (please specify below)	<input type="checkbox"/>	<input type="checkbox"/>
	<input type="checkbox"/>	<input type="checkbox"/>
	<input type="checkbox"/>	<input type="checkbox"/>
	<input type="checkbox"/>	<input type="checkbox"/>
	<input type="checkbox"/>	<input type="checkbox"/>
	<input type="checkbox"/>	<input type="checkbox"/>

## 22. Chief Investigator and Head of Department Declaration

Please note that unsigned applications will not be accepted and both signatures are required

I have read the University's Code of Practice on Investigations involving Human Beings and have completed this application accordingly.

Signature of Chief Investigator



Please also type name here:

Stephan Solomonidis

I confirm I have read this application, I am happy that the study is consistent with departmental strategy, that the staff and/or students involved have the appropriate expertise to undertake the study, that the study makes appropriate use of available resources and facilities within the department and that there are no other departmental-specific issues relating to the study of which I am aware

Signature of Head of Department



Date:

30 / 07 / 2013

23. Only for University sponsored projects under the remit of the DEC/SEC, with no external funding and no NHS involvement

**Head of Department statement on Sponsorship**

This application requires the University to sponsor the investigation. This is done by the Head of Department for all DEC applications with exception of those that are externally funded and those which are connected to the NHS (those exceptions should be submitted to R&KES). I am aware of the implications of University sponsorship of the investigation and have assessed this investigation with respect to sponsorship and management risk. As this particular investigation is within the remit of the DEC and has no external funding and no NHS involvement, I agree on behalf of the University that the University is the appropriate sponsor of the investigation and there are no management risks posed by the investigation.

If not applicable, click here

Signature of Head of Department



Date:

30 / 07 / 2013

For applications to the University Ethics Committee the completed form should be sent to [ethics@strath.ac.uk](mailto:ethics@strath.ac.uk) with the relevant electronic signatures.

## **Management Risk Assessment and Sponsorship**

The Code of Practice on Investigations involving Human Beings requires that all investigations involving humans as subjects should be subject to management risk assessment as well as ethical scrutiny. For those investigations that fall within the remit of the University Ethics Committee, and/or involve the NHS, and/or are externally funded then this form should be completed and submitted to Research & Knowledge Exchange Services. For those investigations that fall within the remit of the Departmental Ethics Committee, and do not involve the NHS, and are not externally funded then this form should be completed and submitted by the Chief Investigator to his/her Head of Department.

1. Title of investigation Locating the Hip Joint using Ultrasonic Techniques
2. Chief Investigator : Stephanos Solomonidis
3. Is it proposed the University will sponsor the investigation (i.e. have responsibility for overall management of the investigation)?  
Yes  No  If no, who is the Sponsor? .....
4. Are you aware of any issues relevant to the University's insurance cover? For example is this a clinical trial and/or are you offering no-fault compensation to volunteers?  
Yes  No   
If yes, what are those issues? .....
5. Are you aware of any issues relevant to the University's assessment of management risk of this project? Please see attached for examples of possible management risk issues.  
Yes  No   
If yes, what are those issues? .....

Signature of Chief Investigator: Stephanos Solomonidis

Date: June 18<sup>th</sup> 2013

For investigations that fall within the remit of the University Ethics Committee, and/or involve the NHS, and/or are externally funded please send this completed form with the appropriate ethics application form to [Helen Baigrie](#), Contracts Manager, Research and Knowledge Exchange Services.

## Participant Information and Consent Forms

# Participant Information Sheet

Name of department: Biomedical Engineering

Title of the study: Locating the Hip joint using Ultrasound Techniques



### Introduction

My name is Mona and I am currently a MSc Biomedical Engineering student at the University of Strathclyde. For my MSc thesis project, I will be looking into the use of an ultrasound device to help assist in locating the hip joint.

### What is the purpose of this investigation?

The purpose of this project is to come up with alternative techniques in locating the hip joint. An ultrasound device will be primarily looked into. The 2D images collected from an ultrasound would be processed to produce 3D images so that a comparison can be made with current practices that are being used in clinical practices to determine their accuracy.

### Do you have to take part?

Participation in this research project is completely voluntary. You have the right to say no. You may change your mind at any time and withdraw. You may choose to stop participating at any time and can choose to withdraw your data at any time. Whether you choose to participate or not will have no effect on your standing at the University of Strathclyde.

### What will you do in the project?

You will be required to lie still on a bed. Ultrasonic gel will then be placed and spread across your hip area. An ultrasound probe will be externally positioned around your hip area. The probe will be used to go around your hip area only; no other areas of your body will be scanned. As the probe will be moved across your hip region, ultrasound images can be simultaneously viewed by both you and the researcher in real time on the ultrasound screen.

The experiments will be held in the biomedical engineering gait laboratory in the month of July. None of the 14 trials conducted should last longer than 5 minutes, allowing you to take breaks in-between the trials if you require.

### Why have you been invited to take part?

Individuals who are classified as obese cannot partake in this experiment due to a higher incorporation of soft tissue artefact. In order to determine whether you qualify, your height in meters and mass in kilograms will be taken. Your mass to height ratio will then be calculated to determine your Body Mass Index (BMI). If your BMI falls between 18.2-25 then you will be able to participate in the experiment.

### What are the potential risks to you in taking part?

No risks are known to be associated with using an ultrasound. No diet or exercise is required for preparation. You will be required to change into shorts before the experiment can be conducted. In the case where something unusual is detected on your ultrasound images, you will be referred to your GP.

### What happens to the information in the project?

No name would be used to store the data. An alphabetical letter will be assigned to you. All data obtained will be logged under and referred to that letter. The images obtained from the ultrasound device will be stored on an encrypted flash drive, accessed only by a password. The chief investigator and researcher will only have access to this flash. Once the project is complete the images will be stored on an encrypted disc.

The University of Strathclyde is registered with the Information Commissioner's Office who implements the Data Protection Act 1998. All personal data on participants will be processed in accordance with the provisions of the Data Protection Act 1998.

Thank you for reading this information – please ask any questions if you are unsure about what is written here.

**What happens next?**

The images obtained from the ultrasound device will be published in a MSc thesis project. An overview of how the images helped in locating the hip joint can be provided if desired. No feedback will be provided based on the images obtained; however, if anything unusual is found on your ultrasound images, you will be referred to your GP.

If you wish to volunteer for this project, please sign the consent form provided. If, however, you are not interested, thank you for your attention.

**Researcher Contact Details:**

Mona Tahvildar-Khazaneh  
Postgraduate: MSc Biomedical Engineering  
Biomedical Engineering  
University of Strathclyde  
106 Rottenrow,  
Glasgow G4 0NW  
Telephone: [REDACTED]  
Email: [REDACTED]

**Chief Investigator Details:**

Stephan Solomonidis  
Biomedical Engineering  
University of Strathclyde  
106 Rottenrow,  
Glasgow G4 0NW  
Telephone: [REDACTED]  
Fax: [REDACTED]  
Email: [REDACTED]

This investigation was granted ethical approval by the Department of Biomedical Engineering Ethics Committee.

If you have any questions/concerns, during or after the investigation, or wish to contact an independent person to whom any questions may be directed or further information may be sought from, please contact:

**Linda Gilmour**

Departmental Ethics Committee  
National Centre for Prosthetics and Orthotics  
Department of Biomedical Engineering  
University of Strathclyde, Curran Building  
131 St James Road  
Glasgow G4 0LS  
Telephone: [REDACTED]  
Email: [REDACTED]

# Consent Form



**Name of department: Biomedical Engineering**

**Title of the study: Locating the Hip joint using Ultrasound Techniques**

- I confirm that I have read and understood the information sheet for the above project and the researcher has answered any queries to my satisfaction.
- I understand that my participation is voluntary and that I am free to withdraw from the project at any time, without having to give a reason and without any consequences.
- I understand that I can withdraw my data from the study at any time.
- I understand that any information recorded in the investigation will remain confidential and no information that identifies me will be made publicly available.
- I consent to being a participant in the project

[Redacted]	Hereby agree to take part in the above project
Signature of Participant:	[Redacted]

## **E-mail: Nature of Participant**

Subject: Participant invited for a biomedical engineering study

Are you aged 20 and over?

We need you for a study to examine the use of different ultrasonic techniques for determining the Hip Joint Centre. For this experiment you will be asked to change into shorts while we scan your hip area. During the scanning time you will be required to lie on a bed for no more than 5 minutes between trials.

You would need to be available for a total of 5 days in the month of July.

To take part please read the attached participant information sheet and sign the consent form.. Return the consent form to Mona Tahvildar-Khazaneh at [REDACTED] detailing your age, height and weight.

Your help will be greatly appreciated.



## Appendix B: MATLAB code

The Following section provides the MATLAB code for locating the HJC based on Gamage and Lasenby's Functional Method developed by Dr. Davydov. The functions that are called for in the main script have also been provided.

### Script

```
%% clean the workspace
hold off
clear all
close all

flag = 2; %1 for mechanical part, 2 for subject data
number_tracks = 4; %number of thigh tracks
split_flag = 0; %change to 1 to do splitting
track_centre = 0;
subjectCraig = 0; % change to 1 if Craig's subject with MRI etc
centre estimates

if flag == 1

    %% load the data:
    % the matrix P of all points and indices of the tracks

    %% extract tracks
    % thigh tracks
    % T(:, :, 1)=P(:, T1ind);
    for i=1:number_tracks
        T(:, :, i)=P(:, eval(['T', int2str(i), 'ind']));
    end
    % hip tracks
    H(:, :, 1)=P(:, H1ind);
    H(:, :, 2)=P(:, H2ind);
    H(:, :, 3)=P(:, H3ind);

    % centre in absolute coordinates
    CE = H(:, :, 1);

    %% coordinate transformation
    % compute the coordinate vectors using the hip tracks
    [s1 s2 s3] = coordinate_vectors (H(:, :, 1), H(:, :, 2), H(:, :, 3));

elseif flag == 2

%Mona's data
Mona_trial_2
number_tracks = 4;
```

```

%% extract tracks
% thigh tracks
% T(:, :, 1)=P(:, T1ind);
for i=1:number_tracks
    T(:, :, i)=P(:, eval(['T', int2str(i), 'ind']));
end

% hip tracks
F1=P(:, F1ind);
F2=P(:, F2ind);
R1=P(:, R1ind);
R2=P(:, R2ind);

% centre of the relative ("hip") coordinate system in absolute
coordinates
CE=F1;

%% coordinate transformation
% compute the coordinate vectors using the hip tracks
[s1 s2 s3] = coordinate_vectors_hip (F1,F2,R1,R2);
[s1 s2 s3] = coordinate_vectors (F1,F2,R1);

end

% transform the thigh tracks into the relative coordinate system
for i=1:number_tracks
    Pr(:, 3*i-2:3*i) = relative_coordinates (T(:, :, i), CE, s1, s2, s3);
%T(:, :, i); %to use absolute coordinates
end

% splitting
if split_flag == 1
%     %split in two
%     Pr = [Pr(1:456, :) Pr(457:912, :)];

%split in three
    Pr = [Pr(1:304, :) Pr(305:608, :) Pr(609:912, :)];

%     %split in three and remove some points
%     Pr = [Pr(1:300, :) Pr(301:600, :) Pr(601:900, :)];
end

disp(' ')

% provide comparison to centres obtained by Craig using
alternative methods
if subjectCraig == 1
%centre computed by Harrington RE
Char = [-55.24; -84.15; -34.35];
%centre computed by Ultrasound
Cult = [-55.51; -72.14; -25.0];
%centre computed by MRI
Cmri = [-39.47; -105.52; -22.92];

```

```

disp('centre estimated by alternative methods:')
disp('Harrington Ultrasound MRI')
disp([Char Cult Cmri])

%estimate the radii of the spheres and accuracy of the sphere fit
using the Harrington RE centre
n=size(Pr,1); % number of points
for i=1:number_tracks
    tmp = Pr(:,3*i-2:3*i) - ones(n,1)*Char';
    tmp = tmp.*tmp;
    tmp = sqrt(sum(tmp'));
    rh(i) = sum(tmp')/length(tmp);
end
disp('radii estimated from Harrington RE centre:')
disp(rh)
disp('Accuracy of the sphere fit for each track and distances to
the centre for Harrington RE')
disp('          rms error  ave_dist  min_dist  max_dist')
n=size(Pr,1); % number of points
for i=1:number_tracks
    diffs = Pr(:,3*i-2:3*i) - ones(n,1)*Char';
    dists = sqrt(sum(diffs.*diffs,2)); %distances to the computed
centre
    ave_dist = sum(dists)/length(dists);
    max_dist = max(dists);
    min_dist = min(dists);
    rad_rms = sqrt(sum((dists - rh(i)).^2)/n);
    disp([int2str(i), '-th track: ', num2str(rad_rms, '%.4f'), ...
        ' ', num2str(ave_dist, '%.4f'), ' ',
        num2str(min_dist, '%.4f'), ' ', num2str(max_dist, '%.4f')])
end

disp(' ')

%estimate the radii of the spheres and accuracy of the sphere fit
using the Ultrasound centre
n=size(Pr,1); % number of points
for i=1:number_tracks
    tmp = Pr(:,3*i-2:3*i) - ones(n,1)*Cult';
    tmp = tmp.*tmp;
    tmp = sqrt(sum(tmp'));
    ru(i) = sum(tmp')/length(tmp);
end
disp('radii estimated from Ultrasound centre:')
disp(ru)
disp('Accuracy of the sphere fit for each track and distances to
the centre for Ultrasound')
disp('          rms error  ave_dist  min_dist  max_dist')
n=size(Pr,1); % number of points
for i=1:number_tracks
    diffs = Pr(:,3*i-2:3*i) - ones(n,1)*Cult';
    dists = sqrt(sum(diffs.*diffs,2)); %distances to the computed
centre
    ave_dist = sum(dists)/length(dists);
    max_dist = max(dists);

```

```

        min_dist = min(dists);
        rad_rms = sqrt(sum((dists - ru(i)).^2)/n);
        disp([int2str(i), '-th track:      ', num2str(rad_rms, '%.4f'), ...
              '      ', num2str(ave_dist, '%.4f'), '
', num2str(min_dist, '%.4f'), '      ', num2str(max_dist, '%.4f')]
end

disp(' ')

%estimate the radii of the spheres and accuracy of the sphere fit
using the MRI centre
n=size(Pr,1); % number of points
for i=1:number_tracks
    tmp = Pr(:,3*i-2:3*i) - ones(n,1)*Cmri';
    tmp = tmp.*tmp;
    tmp = sqrt(sum(tmp'));
    rm(i) = sum(tmp')/length(tmp);
end
disp('radii estimated from MRI centre:')
disp(rm)
disp('Accuracy of the sphere fit for each track and distances to
the centre for MRI')
disp('          rms error  ave_dist   min_dist   max_dist')
n=size(Pr,1); % number of points
for i=1:number_tracks
    diffs = Pr(:,3*i-2:3*i) - ones(n,1)*Cmri';
    dists = sqrt(sum(diffs.*diffs,2)); %distances to the computed
centre
    ave_dist = sum(dists)/length(dists);
    max_dist = max(dists);
    min_dist = min(dists);
    rad_rms = sqrt(sum((dists - rm(i)).^2)/n);
    disp([int2str(i), '-th track:      ', num2str(rad_rms, '%.4f'), ...
          '      ', num2str(ave_dist, '%.4f'), '
', num2str(min_dist, '%.4f'), '      ', num2str(max_dist, '%.4f')]
end
end

%return

%compute the centre by using the two "ball tracks" (Taranjit's
"new" mechanical model data)
if track_centre == 1
    %compute absolute coordinates of the centre
    C1 = P(:,C1ind);
    C2 = P(:,C2ind);
    Ca=(C1+C2)/2;

% %debugging
% disp('centre in absolute coordinates estimated from ball
markers:')
% disp('      average      minimum      maximum      max-min')
% disp([sum(Ca)/size(Ca,1); min(Ca); max(Ca); max(Ca)-min(Ca)])

% plot the original ball tracks in absolute coordinates

```

```

figure(100)
plot3(C1(:,1),C1(:,2),C1(:,3),'.')
hold on
plot3(C2(:,1),C2(:,2),C2(:,3),'.')
plot3(Ca(:,1),Ca(:,2),Ca(:,3),'r.')
axis equal
axis tight

%transform the ball tracks and centre into relative coordinates
C1r=relative_coordinates (C1,CE,s1,s2,s3);
C2r=relative_coordinates (C2,CE,s1,s2,s3);
Cr=relative_coordinates (Ca,CE,s1,s2,s3);

%% plot the ball tracks in relative coordinates
figure(101)
plot3(C1r(:,1),C1r(:,2),C1r(:,3),'.')
hold on
plot3(C2r(:,1),C2r(:,2),C2r(:,3),'.')
plot3(Cr(:,1),Cr(:,2),Cr(:,3),'r.')
axis equal
axis tight

disp('centre estimated from ball markers:')
disp('  average  minimum  maximum  max-min')
Cr_ave = sum(Cr)/size(Cr,1);
disp([Cr_ave; min(Cr); max(Cr); max(Cr)-min(Cr)])

%estimate the radii of the spheres using the centre from "ball
tracks"
for i=1:number_tracks
    tmp = Pr(:,3*i-2:3*i) -Cr;
    tmp = tmp.*tmp;
    tmp = sqrt(sum(tmp'));
    rb(i) = sum(tmp')/length(tmp);
end
disp('radii estimated from ball markers:')
disp(rb)
disp('Accuracy of the ball marker sphere fit for each track and
distances to the centre')
disp('          rms error    bias    ave_dist    min_dist
max_dist')
n=size(Pr,1); % number of points
for i=1:number_tracks
    diffs = Pr(:,3*i-2:3*i) - ones(n,1)*Cr_ave;
    dists = sqrt(sum(diffs.*diffs,2)); %distances to the computed
centre
    ave_dist = sum(dists)/length(dists);
    max_dist = max(dists);
    min_dist = min(dists);
    rad_rms = sqrt(sum((dists - rb(i)).^2)/n);
    rad_bias = sum(dists)/n - rb(i);
    disp([int2str(i),'-th track:    ',num2str(rad_rms,'% .4f'),'
',num2str(rad_bias,'% .2e'),...
        '    ',num2str(ave_dist,'% .4f'),'
',num2str(min_dist,'% .4f'),'    ',num2str(max_dist,'% .4f')])
end

```

```

end

% find the centre of rotation and radii
[c r A b] = GamageLasenby(Pr);
disp(' ')
disp('centre estimated by Gamage/Lasenby:')
disp(c)
disp('radii estimated by Gamage/Lasenby:')
disp(r)

if track_centre == 1
    disp('difference between centre estimated by ball markers and
Gamage/Lasenby:')
    disp([sum(Cr)/size(Cr,1)]'-c)
    disp('difference between radii estimated by ball markers and
Gamage/Lasenby:')
    disp(rb-r)
end

%% generate the spheres
% points of the unit sphere
[X,Y,Z] = sphere(20);
% expand to the radius r and shift to the centre c
for i=1:number_tracks
    XX(:, :, i) = X*r(i) + c(1);
    YY(:, :, i) = Y*r(i) + c(2);
    ZZ(:, :, i) = Z*r(i) + c(3);
end

%% plot some of the original thigh tracks
figure(1)
for i=1:2
    plot3(T(:,1,i),T(:,2,i),T(:,3,i),'.')
    hold on
    axis equal
end
axis tight

%% plot all thigh data in relative coordinates
figure(2)
hold on
for i=1:number_tracks
    plot3(Pr(:,3*i-2),Pr(:,3*i-1),Pr(:,3*i),'.')
end
axis equal
axis tight

%% plot each thigh track with the sphere
for i=1:number_tracks
    figure
    plot3(Pr(:,3*i-2),Pr(:,3*i-1),Pr(:,3*i),'.')
    hold on

```

```

        mesh(XX(:,:,i),YY(:,:,i),ZZ(:,:,i))
    axis equal
    axis tight
end

%% Assesment
disp(['condition number of A: ',num2str(cond(A))])
disp(' ')
disp('Accuracy of the sphere fit for each track and distances to
the centre for Gamage/Lasenby')
disp('          rms error      bias      ave_dist      min_dist
max_dist')
n=size(Pr,1); % number of points
for i=1:number_tracks
    diffs = Pr(:,3*i-2:3*i) - ones(n,1)*c';
    dists = sqrt(sum(diffs.*diffs,2)); %distances to the computed
centre
    ave_dist = sum(dists)/length(dists);
    max_dist = max(dists);
    min_dist = min(dists);
    rad_rms = sqrt(sum((dists - r(i)).^2)/n);
    rad_bias = sum(dists)/n - r(i);
    disp([int2str(i),'-th track: ',num2str(rad_rms,'% .4f'),'
',num2str(rad_bias,'% .2e'),...
        '          ',num2str(ave_dist,'% .4f'),'
',num2str(min_dist,'% .4f'),'          ',num2str(max_dist,'% .4f')])
end

if flag == 1

    %% plot all hip tracks and the track of the computed centre
    figure
    hold on
    for i=1:3
        plot3(H(:,1,i),H(:,2,i),H(:,3,i),'.')
    end
    cabs = absolute_coordinates (ones(n,1)*c',CE,s1,s2,s3);
    plot3(cabs(:,1),cabs(:,2),cabs(:,3),'r')
    axis equal
    axis tight

end
disp(' ')

% %% plot the hip data in relative coordinates (needed for
debugging only)
% each track must collapse into one point
% figure(356)
% for i=5:7
%     Pr(:,3*i-2:3*i) = relative_coordinates (P(:,3*i-
2:3*i),H(:,:,1),s1,s2,s3);
%     plot3(Pr(:,3*i-2),Pr(:,3*i-1),Pr(:,3*i),'r')
%     hold on
% end
% axis equal

```

```
% axis tight
```

```
Relative Coordinates
```

```
function pnew = relative_coordinates (p,c,s1,s2,s3)
% given n points in absolute coordinates and the relative
coordinate system for each,
% compute the relative coordinates of all points
% p - an (n x 3)-matrix whose rows are absolute coordinates to
be transformed
% c - an (n x 3)-matrix whose rows are absolute coordinates of
the origins of the
% relative coordinate systems
% s1,s2,s3 - (n x 3)-matrices of unit vectors of the relative
coordinate systems
% pnew - the (n x 3)-matrix of relative coordinates
%
% Oleg Davydov 02/06/2010
```

```
% the coordinates are the inner products of p-c with s1,s2,s3
p=p-c;
pnew = [sum(p.*s1,2) sum(p.*s2,2) sum(p.*s3,2)] ;
```

### **Rotation Matrix**

```
function R=rotation_matrix3D(a,b,c)
%3D rotation matrix with Euler angles a,b,c
%http://en.wikipedia.org/wiki/Rotation\_matrix

Rx=[1 0 0; 0 cos(b) -sin(b); 0 sin(b) cos(b)];
Ry=[cos(a) 0 sin(a); 0 1 0; -sin(a) 0 cos(a)];
Rz=[cos(c) -sin(c) 0; sin(c) cos(c) 0; 0 0 1];
R=Rz*Rx*Ry;
```

### **Coordinate Vector Hip**

```
function [s1 s2 s3] = coordinate_vectors_hip (f1,f2,r1,r2)
% computes three arrays of unit coordinate vectors from three
arrays of 3D points
% f1,f2,r1,r2 - (n x 3)-matrices containing for each n the
coordinates of the two front (f1,f2)
% and two rear (r1,r2) markers on the hip
% s1,s2,s3 - (n x 3)-matrices containing for each n the
coordinates of three unit vectors that
% build an orthogonal coordinate system generated by
orthogonalising p2-p1 and p3-p1,
% and adding their cross product
% The origins of the new coordinate systems will be at f1
% Assumes that the points in the rows of p1,p2,p3 are not
collinear
```



```

%
% Oleg Davydov 25/07/2010

%% compute the third coordinate directions (z-axis) as difference
of f2 and f1
z=f1-f2;
z=normalise(z); %normalisation

%% compute the first coordinate directions (x-axis)
x=(f1+f2-r1-r2)/2;

% orthogonalise x to z; comment out the next two lines to discard
orthogonalisation
pr = sum(x.*z,2); % compute projections on z
x=x-z.*pr(:, [1 1 1]);% orthogonalisation of x

%normilise x
x=normalise(x);

%% compute the second coordinate directions (y-axis) using the
cross product
y = cross(z,x,2);
y=normalise(y);

s1=x;
s2=y;
s3=z;

% %debugging: check orthogonality
% xz= max(abs(sum(x.*z,2)))
% xy =max(abs(sum(x.*y,2)))
% zy =max(abs(sum(z.*y,2)))

function v = normalise(v)
% normalise each row of an (n x 3)-matrix

norms = sqrt(sum(v.*v,2));
v=v./norms(:, [1 1 1]);
%v=v./norms(:,ones(3, 1));

```

### **Coordinate Vector**

```

function [s1 s2 s3] = coordinate_vectors (p1,p2,p3)
% computes three arrays of unit coordinate vectors from three
arrays of 3D points
% p1,p2,p3 - (n x 3)-matrices containing for each n the
coordinates of three points in the space
% s1,s2,s3 - (n x 3)-matrices containing for each n the
coordinates of three unit vectors that
%
%           build an orthogonal coordinate system generated by
orthogonalising p2-p1 and p3-p1,
%
%           and adding their cross product
% The origins of the new coordinate systems will be at p1

```

```

% Assumes that the points in the rows of p1,p2,p3 are not
collinear
%
% Oleg Davydov 04/06/2010

%% compute the first coordinate directions as difference of p2 and
p1
s1=p2-p1;
s1=normalise(s1); %normalisation

%% compute the second coordinate directions by orthogonalising the
difference p3-p1
s2=p3-p1;
pr = sum(s2.*s1,2); % compute projections on s1
s2=s2-s1.*pr(:, [1 1 1]);% orthogonalisation of s2
s2=normalise(s2);

% compute the third coordinate directions using the cross product
s3 = cross(s1,s2,2);
s3=normalise(s3);

function v = normalise(v)
% normalise each row of an (n x 3)-matrix

norms = sqrt(sum(v.*v,2));
v=v./norms(:, [1 1 1]);
%v=v./norms(:,ones(3, 1));

```

### **Absolute Coordinate**

```

function pnew = absolute_coordinates (p,c,s1,s2,s3)
% given n points in relative coordinates and the relative
coordinate system for each,
% compute the absolute coordinates of all points
% p -- an (n x 3)-matrix whose rows are relative coordinates to
be transformed
% c -- an (n x 3)-matrix whose rows are absolute coordinates of
the origins of the
% relative coordinate systems
% s1,s2,s3 -- (n x 3)-matrices of unit vectors of the relative
coordinate systems
% pnew -- the (n x 3)-matrix of absolute coordinates
%
% Oleg Davydov 04/06/2010

% for each moment, the transformation matrix is the transpose of
the matrix given by s1,s2,s3,
% and the coordinates of the absolute unit vectors are the columns
of this matrix:
t1 = [s1(:,1) s2(:,1) s3(:,1)];
t2 = [s1(:,2) s2(:,2) s3(:,2)];
t3 = [s1(:,3) s2(:,3) s3(:,3)];

```

```

% find the relative coordinates of the origin of the absolute
system
cnew = -[sum(c.*s1,2) sum(c.*s2,2) sum(c.*s3,2)];

% the coordinates are the inner products of p-cnew with t1,t2,t3
p=p-cnew;
pnew = [sum(p.*t1,2) sum(p.*t2,2) sum(p.*t3,2)];

```

### **Gamage and Lasenby**

```

function [c r A b] = GamageLasenby(P)
% Computing the centre of rotation from a number of tracks on
concentric spheres
%
% Reads a matrix P of size n x 3p, where p is the number of tracks
% and n the number of points in each track.
% In each track, the three consecutive columns correspond to x-,
y- and z-coordinates.
%
% Returns:
%   c -- the coordinates of the centre of rotation
%   r -- the p-vector of radii of the spheres of the tracks
%   A,b -- the matrix and RHS of the linear system to investigate
numerical stability
%
% Oleg Davydov 04/06/2010

% number of points in the tracks
n = size(P,1);

% number of tracks
p = size(P,2)/3;

%% various averages and outer products for all tracks
av = reshape(mean(P),3,[]);
PP = P.*P; % squares of all entries of P
%av2 = sum(reshape(sum(PP),3,[]))/n;
av2 = zeros(1,p);
av3 = zeros(3,p);
Avop = zeros(3,3*p); %outer products of averages
Pt=P';
Pop=zeros(3*n,3*p); % outer products of the points in 3x3-blocks
for i=1:p
    indx = 3*i-2:3*i;
    sqn=sum(PP(:,indx),2);% squared norms of all points of the p-th
track
    av2(i) = sum(sqn)/n;
    av3(:,i) = sum(P(:,indx).*sqn(:,[1 1 1]))'/n;
    tav = av(:,i);
    Avop(:,indx)=tav*tav';
    Pop(:,indx(1))=reshape(Pt(indx,:),3*n,1);
    Pop(:,indx(2))=reshape(Pt(indx,:),3*n,1);
    Pop(:,indx(3))=reshape(Pt(indx,:),3*n,1);

```

```

end
Pop=Pop.*P(reshape([1:n; 1:n; 1:n],3*n,1),:); % contains the outer
products in 3x3-blocks

%% setting up the linear system
% RHS
b = sum(av3 - av.*av2([1; 1; 1],:),2);
% sum up the outer product matrices in columns, average and
subtract the matrix avop
Sop=[sum(Pop(1:3:3*n-2,:)); sum(Pop(2:3:3*n-1,:));
sum(Pop(3:3:3*n,:))]/n - Avop;
% sum up in rows to obtain the matrix of the linear system
A=2*[sum(Sop(:,1:3:3*p-2),2) sum(Sop(:,2:3:3*p-1),2)
sum(Sop(:,3:3:3*p),2)];

% solve the linear system to obtain the centre or rotation
c=A\b;

% find the radii
P=P-c(ones(n,1)*reshape([ones(1,p); 2*ones(1,p);
3*ones(1,p)],1,3*p));
P = P.*P;
r = sqrt(sum(reshape(sum(P),3,p))/n);

```

## Appendix C: Ultrasound Image Modification

This section details the modifications that were made to the ultrasound images obtained from the Toshiba SSA-325A for importation into the Mimics 12.01 software.

An example of an original ultrasound image taken from the phantom femur model surrounded by tissue mimicking material. The MPEG video taken of the model was first converted into a series of pictures using the snap shot feature in the VLC program and was then saved as PNG.

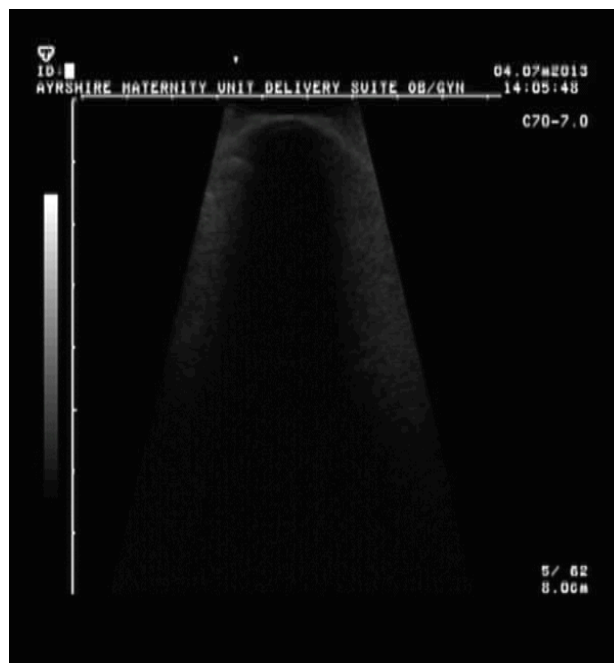


*Figure A. 1: Ultrasound Image before Modification*

Sample of the original ultrasound image after being cropped and compressed into JPEG and BMP file format.

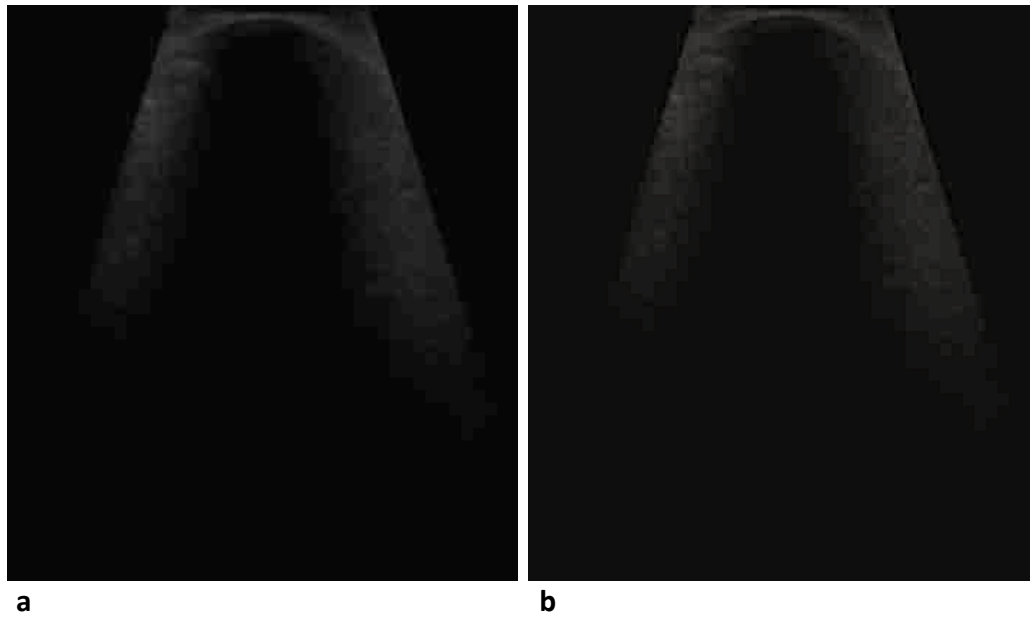


*Figure A. 2: Ultrasound Images after Modification (a) JPEG (b) BMP*

The following table lists the properties of the modified ultrasound images.

*Table A. 1: Properties of Ultrasound Images*

	<b>Before Modification</b>	<b>After Modification</b>	
<b>Format</b>	Portable Network Graphics Image (PNG)	JPEG	Bitmap (BMP)
<b>Size</b>	82KB	850KB	450KB
<b>Dimension</b>	640 x 480	394 x 387	394 x 387

## **Appendix D: Re-sizing Image MATLAB Code**

The following section provides the MATLAB code used for re-sizing the BMP ultrasound images obtained from the Toshiba SSA-325A.

### **Script**

```
I_new = imresize(I, [380 345])
```